

CAPITAL UNIVERSITY OF SCIENCE AND
TECHNOLOGY, ISLAMABAD



**Study of Essential Oil of Different
Spices as Inhibitor of 3CL
Protease of SARS-CoV-2**

by

Attia Saif

A thesis submitted in partial fulfillment for the
degree of Master of Science

in the

Faculty of Health and Life Sciences

Department of Bioinformatics and Biosciences

2022

Copyright © 2022 by Attia Saif

All rights reserved. No part of this thesis may be reproduced, distributed, or transmitted in any form or by any means, including photocopying, recording, or other electronic or mechanical methods, by any information storage and retrieval system without the prior written permission of the author.

Every challenging work needs self-efforts as well as the guidance of elders. I dedicate this thesis to my parents whose affection makes me able to get such success and to my teachers whose encouragement has always been my source of inspiration.



CERTIFICATE OF APPROVAL

Study of Essential Oil of Different Spices as Inhibitor of 3CL Protease
of SARS-CoV-2

by

Attia Saif

(MBS203023)

THESIS EXAMINING COMMITTEE

S. No.	Examiner	Name	Organization
(a)	External Examiner	Dr. Rida Saeed	NUMS, Rawalpindi
(b)	Internal Examiner	Dr. Arshia Amin Butt	CUST, Islamabad
(c)	Supervisor	Dr. Erum Dilshad	CUST, Islamabad

Dr. Erum Dilshad

Thesis Supervisor

November, 2022

Dr. Syeda Marriam Bakhtiar

Head

Dept. of Bioinformatics & Biosciences

November, 2022

Dr. Sahar Fazal

Dean

Faculty of Health & Life Sciences

November, 2022

Author's Declaration

I, **Attia Saif** hereby state that my MS thesis titled “**Study of Essential Oil of Different Spices as Inhibitor of 3CL Protease of SARS-CoV-2**” is my own work and has not been submitted previously by me for taking any degree from Capital University of Science and Technology, Islamabad or anywhere else in the country/abroad.

At any time if my statement is found to be incorrect even after my graduation, the University has the right to withdraw my MS Degree.

(**Attia Saif**)

Registration No: MBS203023

Plagiarism Undertaking

I solemnly declare that research work presented in this thesis titled “**Study of Essential Oil of Different Spices as Inhibitor of 3CL Protease of SARS-CoV-2**” is solely my research work with no significant contribution from any other person. Small contribution/help wherever taken has been dully acknowledged and that complete thesis has been written by me.

I understand the zero tolerance policy of the HEC and Capital University of Science and Technology towards plagiarism. Therefore, I as an author of the above titled thesis declare that no portion of my thesis has been plagiarized and any material used as reference is properly referred/cited.

I undertake that if I am found guilty of any formal plagiarism in the above titled thesis even after award of MS Degree, the University reserves the right to withdraw/revoke my MS degree and that HEC and the University have the right to publish my name on the HEC/University website on which names of students are placed who submitted plagiarized work.

(Attia Saif)

Registration No: MBS203023

Acknowledgement

All the praises are to be for Almighty **ALLAH** and **Prophet MUHAMMAD (SAW)**. I would like to express my wholehearted thanks to my family for the generous support throughout of pursuing the MS degree. I am heartily grateful to my supervisor Dr. Erum Dilshad (Assistant professor, Department of Bioinformatics and Biosciences, CUST) for her kind support, guidelines and arrangement of tutorial classes. I am grateful to her for approving research topic, her disciplinarian attitude, and strictness in punctuality and working in organized manner makes possible to complete this work. Not to be forgotten, my friends who helped me morally for accomplishment of this goal. Thanks to all.

(Attia Saif)

Abstract

SARS CoV 2 (severe acute respiratory syndrome coronavirus 2), was first reported in a city of Wuhan, China. The infection rate of the corona virus (SARS-CoV-2) was so high that it infected more than one thousand people in fifteen days. World Health Organization (WHO) has categorized SARS-CoV-2 as a major global threat to humanity due to its high fatality rate, high transmission rate, and increased reproduction. COVID-19 is currently being treated with a variety of small molecule drugs and vaccines. Since the early days of the COVID-19 outbreak, herbal traditional medicines were used in China. Essential oils have long been used for bactericidal, virucidal, fungicidal, anti-parasitic, insecticidal, cosmetic, medicinal, and cosmetic purposes, particularly in the pharmaceutical, sanitary, agricultural, and food industries. Spices have many phytochemicals i.e., alkaloids, glycoside, carbohydrates, saponins, phenols, steroid, tannins, proteins, proteins and diterpenes. The 3-chymotrypsin-like protease (3CLpro) is the main protease of the SARS-CoV-2 that cleaves the large replicase polyproteins during viral replication and therefore considered as an attractive drug target. So, we reported molecular docking-based virtual screening of 5 active compounds each from 10 spices i.e. *Origanum vulgare*, *Piper nigrum*, *Cinnamomum verum*, *Cuminum cyminum* and *Trachyspermum ammi*. Active compounds were taken from Pubchem database. After physiochemical analysis and identification of active domains of 3CLpro, these compounds were docked via CB-Dock to determine the best potential inhibitor against 3CL protease of COVID 19. These 5 compounds from each plant were further subjected to Lipinski rule of five and ADMET properties for drug-likeness prediction. Furthermore, the lead compound was identified with best binding affinity and pharmacological properties. Remdesivir was used as criteria for comparison. These findings suggest that the identified compounds may serve as potential inhibitor against 3CLpro. Hence, gamma-terpineol from *Origanum vulgare*, piperine from *Piper nigrum*, cinnamaldehyde from *Cinnamomum verum*, cuminaldehyde from *Cuminum cyminum*, Terpinene-4-ol from *Trachyspermum ammi* are considered as lead compounds. Comparison of these ligands with Remdesivir shows that they are all recommended as potential inhibitors of 3CLprotease of COVID 19.

Contents

Author's Declaration	iv
Plagiarism Undertaking	v
Acknowledgement	vi
Abstract	vii
List of Figures	xi
List of Tables	xiii
Abbreviations	xv
1 Introduction	1
1.1 Background	1
1.2 Problem Statement	4
1.3 Aims and Objectives	4
2 Review of Literature	5
2.1 SARS-CoV-2	5
2.2 Origin	6
2.3 Entry and Life Cycle	6
2.4 Symptoms	8
2.5 Statistics	8
2.6 Treatment	9
2.7 Medicinal Plants	11
2.8 Essential Oils	12
2.8.1 Essential Oil of <i>Origanum vulgare</i>	13
2.8.2 Essential Oil of <i>Piper nigrum</i>	13
2.8.3 Essential Oil of <i>Cinnamomum verum</i>	13
2.8.4 Essential Oil of <i>Cuminum cyminum</i>	14
2.8.5 Essential Oil of <i>Trachyspermum ammi</i>	14
2.9 Molecular Docking	14
2.10 3CL Pro or Mpro	15

2.11	Natural Compounds as Inhibitors of 3CL Protease	16
3	Research Methodology	17
3.1	Methodology Flowchart	17
3.2	Selection of Disease	18
3.3	Selection of Protein	18
3.4	Determination of Physiochemical Properties of Proteins	18
3.5	Cleaning of the Downloaded Protein	19
3.6	Determination of Functional Domains of Target Proteins	19
3.7	Selection of Active Metabolic Ligands	19
3.8	Ligand Preparation	19
3.9	Molecular Docking	20
3.10	Visualization of Docking Result Via PyMol	20
3.11	Analysis of Docked Complex Via LigPlot	21
3.12	Ligand ADMET Properties	21
3.13	Lead Compound Identification	21
3.14	Comparison of Antiviral Drug Against COVID- 19 and Lead Compound	22
4	Results and Discussions	23
4.1	Sequence Retrieval of Protein	23
4.2	Analysis of Physiochemical Properties of 3CL Protease	24
4.3	Identification of Functional Domains	25
4.4	Structure of Protein Cleaned for Docking	26
4.5	Ligand Selection	27
4.6	Virtual Screening	31
4.7	Molecular Docking	33
4.8	Interaction of Ligands and Targeted Protein	36
4.9	ADMET Properties of Ligands	56
4.9.1	Absorption	57
4.9.2	Distribution	60
4.9.3	Metabolism	62
4.9.4	Excretion	66
4.9.5	Toxicity	67
4.10	Lead Compound Identification	72
4.11	Selection of Antiviral Drug	72
4.12	Mechanism of Action of Remdesivir	73
4.13	Remdesivir Effects on Body	73
4.14	ADMET Properties of Selected Drug	74
4.15	Remdesivir Docking	78
4.16	Comparison of Remdesivir and Best Ligand	79
4.16.1	Comparison of Physiochemical Properties and ADMET Properties	79
4.16.2	Comparison of Docking Results	86

5 Conclusions and Recommendations	87
Bibliography	88

List of Figures

2.1	Structure of SARS-CoV-2	5
2.2	Severe Acute Respiratory Syndrome Coronavirus 2 (SARS-CoV-2) Lifecycle	7
2.3	Viral vector vaccines	9
2.4	Genetic vaccines	10
2.5	Inactivated vaccines	10
2.6	Protein vaccines	11
2.7	Structure of 3CL protease of SAES-CoV-2	15
3.1	The flowchart of methodology	17
4.1	Structure of 3CL protease from PDB	24
4.2	Functional Domains of 3CL Protease	26
4.3	Refined Structure of 3CLpro for Docking.	26
4.4	2D structure showing interaction of Carvacrol with 3CL pro.	37
4.5	2D structure showing interaction of Thymol with 3CL pro.	37
4.6	2D structure showing interaction of Alpha-terpineol with 3CL pro.	38
4.7	2D structure showing interaction of Gamma-terpineol with 3CL pro.	38
4.8	2D structure showing interaction of Linalool with 3CL pro.	39
4.9	2D structure showing interaction of Beta-caryophyllene with 3CL pro.	39
4.10	2D structure showing interaction of Piperine with 3CL pro.	40
4.11	2D structure showing interaction of Sabinene with 3CL pro.	40
4.12	2D structure showing interaction of Beta-pinene with 3CL pro.	41
4.13	2D structure showing interaction of Alpha-copaene with 3CL pro.	41
4.14	2D structure showing interaction of Cinnamaldehyde with 3CL pro.	42
4.15	2D structure showing interaction of Linalool with 3CL pro.	42
4.16	2D structure showing interaction of Beta-caryophyllene with 3CL pro.	43
4.17	2D structure showing interaction of Eucalyptol with 3CL pro.	43
4.18	2D structure showing interaction of Eugenol with 3CL pro.	44
4.19	2D structure showing interaction of Cuminaldehyde with 3CL pro.	44
4.20	2D structure showing interaction of P-cymene with 3CL pro.	45
4.21	2D structure showing interaction of Gamma-terpinene with 3CL pro.	45
4.22	2D structure showing interaction of Beta-pinene with 3CL pro.	46
4.23	2D structure showing interaction of Thymol with 3CL pro.	46

4.24	2D structure showing interaction of Thymol with 3CL pro.	47
4.25	2D structure showing interaction of Carvacrol with 3CL pro.	47
4.26	2D structure showing interaction of P-cymene with 3CL pro.	48
4.27	2D structure showing interaction of Beta-pinene with 3CL pro.	48
4.28	2D structure showing interaction of Terpinene-4-ol with 3CL pro.	49

List of Tables

2.1	Statistical analysis of Covid-19 cases in Pakistan ad globally.	9
4.1	Physiochemical properties of 3CL protease.	25
4.2	Ligands from <i>Origanum vulgare</i>	27
4.3	Ligands from <i>Piper nigrum</i>	28
4.4	Ligands from <i>Cinnamomum verum</i>	29
4.5	Ligands from <i>Cuminum cyminum</i>	29
4.6	Ligands from <i>Trachyspermum ammi</i>	30
4.7	Selected ligands showing Lipinski rule of five.	31
4.7	Selected ligands showing Lipinski rule of five.	32
4.7	Selected ligands showing Lipinski rule of five.	33
4.8	Docking results of selected ligands.	34
4.8	Docking results of selected ligands.	35
4.8	Docking results of selected ligands.	36
4.9	Selected ligands showing hydrogen bonding and hydrophobic interactions.	49
4.9	Selected ligands showing hydrogen bonding and hydrophobic interactions.	50
4.9	Selected ligands showing hydrogen bonding and hydrophobic interactions.	51
4.9	Selected ligands showing hydrogen bonding and hydrophobic interactions.	52
4.9	Selected ligands showing hydrogen bonding and hydrophobic interactions.	53
4.9	Selected ligands showing hydrogen bonding and hydrophobic interactions.	54
4.9	Selected ligands showing hydrogen bonding and hydrophobic interactions.	55
4.9	Selected ligands showing hydrogen bonding and hydrophobic interactions.	56
4.10	a) Absorptive properties of selected ligands.	57
4.10	a) Absorptive properties of selected ligands.	58
4.11	b) Absorptive properties of selected ligands.	58
4.11	b) Absorptive properties of selected ligands.	59
4.11	b) Absorptive properties of selected ligands.	60
4.12	Distributive properties of selected ligands.	61

4.12	Distributive properties of selected ligands.	62
4.13	Metabolic properties of selected ligands.	63
4.13	Metabolic properties of selected ligands.	64
4.13	Metabolic properties of selected ligands.	65
4.14	Excretory properties of selected ligands.	66
4.14	Excretory properties of selected ligands.	67
4.15	a) Toxicity prediction of selected ligands.	68
4.15	a) Toxicity prediction of selected ligands.	69
4.16	b) Toxicity prediction of selected ligands.	70
4.16	b) Toxicity prediction of selected ligands.	71
4.17	Physiochemical properties of Remdesevir.	72
4.18	Showed the ADMET properties of remdesevir	76
4.18	Showed the ADMET properties of remdesevir	77
4.18	Showed the ADMET properties of remdesevir	78
4.19	Docking result of Remdesevir with 3CL protease.	79
4.20	Comparison of physiochemical and ADMET properties of lead com- pounds and remdesevir.	80
4.20	Comparison of physiochemical and ADMET properties of lead com- pounds and remdesevir.	81
4.20	Comparison of physiochemical and ADMET properties of lead com- pounds and remdesevir.	82
4.20	Comparison of physiochemical and ADMET properties of lead com- pounds and remdesevir.	83
4.20	Comparison of physiochemical and ADMET properties of lead com- pounds and remdesevir.	84
4.20	Comparison of physiochemical and ADMET properties of lead com- pounds and remdesevir.	85
4.21	a) Comparison of docking result of remdesevir and lead compounds.	86
4.22	b) Comparison of docking result of remdesevir and lead compounds.	86

Abbreviations

ADMET: - Absorption, Distribution, Metabolism, Excretion and Toxicity

BBB permeability: - Blood-brain barrier permeability

CADD: - Computer-Assisted Drug Discovery

CB-dock: - Cavity detection guided blind docking

CNS permeability: - Central Nervous System permeability

CoVs: - Coronaviruses

3CL Pro: - 3-chymotrypsin-like protease

HBA: - Hydrogen Bond Acceptor

HBD: - Hydrogen Bond Donor

KEGG: - Kyoto Encyclopedia of Genes and Genomes

M Pro: - Main protease

MERS-CoV: - Middle East Respiratory Syndrome Coronavirus

ORF: - Open Reading Frame

P-glycoprotein: - Permeability glycoprotein

PL Pro: - Papain-like protease

SARS-CoV: - Severe Acute Respiratory Syndrome Coronavirus

SPHEC: - Sixth Public Health Emergency

VDss: - Volume distribution in steady state

WHO: - World Health Organization

Chapter 1

Introduction

1.1 Background

SARS CoV 2 (severe acute respiratory syndrome coronavirus 2), was first reported in a city of Wuhan, China [1]. The infection rate of the corona virus (SARS-CoV-2) was so high that it infected more than one thousand people in fifteen days. Afterwards, the number of infected patients keeps on increasing day by day with a 2-4% mortality rate [2]. The infection was highly contagious because it spreads through the liquid droplets that are produced during coughing and sneezing. The virus could survive for few days in these droplets and spreads quickly via hand to mouth or hand to high contact and contaminated hard metallic surfaces. Therefore, close human contact was prohibited as a first safety precaution from this virus [3].

COVID-19 is a systemic disease that starts from the airway and reaches blood through the lungs. Blood disseminate the virus to the multiple organs among which the nervous system, kidneys, spleen, liver and muscles are more prone to infection [3], [4]. Of note, coronavirus produces mild infection except the few variants (beta SARS-CoV and MERS-CoV) which have caused more deaths [8], [9], [10], [11]. On January 30, 2020, the WHO (World Health Organization) declared the COVID 19 pandemic as the sixth public health emergency (SPHEC)

[5]. However, this was not the coronavirus' first outbreak, previously the "SARS-CoV 1" outbreak in 2002 and the "MERS-CoV" (middle east respiratory syndrome coronavirus) outbreak in 2012 had been reported [6].

"COVID-19" is supposed to be the third coronavirus pandemic that has affected more than 209 countries, including Pakistan. According to WHO, there were a total of 416,614,051 cases reported, with 5,844,097 mortalities to the date, whereas the United States has the highest number of positive coronavirus cases, followed by Italy and Spain (WHO). Coronaviruses are enveloped, non-segmented positive-sense RNA viruses that are widely distributed in humans and other mammals. They belong to the family Coronaviridae and the order Nidovirales [7]. This virus is responsible of encoding twenty different proteins which include four main structural proteins i.e. "S: spike"; "N: nucleocapsid", "E: envelope"; "M: membrane" and some nonstructural proteins such as RNA-dependent RNA polymerase "RdRp", coronavirus main protease "3CLpro", and also papain-like protease "PL-pro" [12]. The enveloped viruses enter the cells via two routes: (1) a "pH-independent receptor-mediated pathway" in which the envelope of the virus attaches with the cell membrane of the host cell to recruit viral de-coating, and (2) a "pH-dependent endocytic pathway" in which clathrin caveolin help the transportation of the virus the endosome "low pH environment" [13] [14]. The first identified passageway for entry of SARS-CoV 2 is the direct fusion through plasma membrane [15]. While some subsequent research has revealed that virus entry may be pH dependent [16].

COVID-19 is currently being treated with a variety of small molecule drugs and vaccines. The World Health Organization (WHO) reported that till September 17, 2020, 36 candidates were in clinical trials to treat COVID-19, and 146 vaccines were in preclinical trials. Granted the ability of vaccines to prevent and treat SARS-CoV-2 infection [17]. The following vaccines have received EUL as of November 26, 2021:

- The "Pfizer/BioNTech Comirnaty", 31 December 2020.
- The "AstraZeneca/AZD1222 vaccines", 16 February 2021.

- The “Janssen” developed by Johnson and Johnson, 12 March 2021.
- The “Moderna COVID-19 vaccine” (mRNA 1273), 30 April 2021.
- The “Sinopharm COVID-19 vaccine”, 7 May 2021.
- The “Sinovac Corona Vac”, 1 June 2021.
- The Bharat Biotech BBV152 COVAXIN vaccine, 3 November 2021. (World Health Organization (WHO) [https://www.who.int/news-room/questions-and-answers-coronavirus-disease-\(covid-19\)-vaccines](https://www.who.int/news-room/questions-and-answers-coronavirus-disease-(covid-19)-vaccines)).

Herbal remedies and natural compounds derived from medicinal plants are good source of inspiration for the development of new antiviral medicines. Some natural drugs have been presented to have antiviral properties against several types of viruses, such as “herpes simplex virus” [18], [19], “influenza virus” [20], “human immunodeficiency virus” [21], “hepatitis B and C viruses” [22], “SARS and MERS” [23]. To combat the global corona crisis, it is necessary to identify and discover new effective antivirals. Many anti-inflammatory and anti-viral natural compounds and their derivatives have a high affinity for 3-chymotrypsin-like protease (3CLpro). For more than three decades, computer-assisted drug discovery “CADD” have been critical in the formation of small molecules that have been therapeutically important. Using computational methods such as molecular docking to screen chemical virtual libraries can save money and time, resulting in faster speeds and the identification of potential drugs. To combat COVID-19, a number of research groups have devised novel policies, such as republishing existing medicines, natural products [24]. Furthermore, enormous efforts had been made in recent years to reveal the antiviral potential of these naturally occurring agents by disturbing the life cycle of the virus at different stages, such as at virus entry, replication, assembly, and release. Also these agents affect the virus-host interactions [25]. The 3CLpro had been proved to be a potential target site in corona virus, the genome sequence has identified that SARS-CoV-2 is very related to SARS-CoV-1, so for COVID-19, the target site for scanning against the natural compounds of herbal medicines is the main protease [26].

1.2 Problem Statement

WHO had categorized SARS-CoV-2 as a major global threat to humanity due to its high fatality rate, high transmission rate, and increased reproduction. The goal of the study was to uprise the information on natural agents which have potential antiviral activity against coronaviruses, as well as to deliberate their molecular goals and mechanisms with least side effects and easy availability. This study will suggest a remedy against COVID 19.

In this study, we targeted the 3CL protease enzyme of the virus with the active compounds having antiviral properties present in essential oils of spices for the conduction of extensive computational studies through molecular docking.

1.3 Aims and Objectives

This study aims to predict the most effective inhibitors present in essential oils of spices against 3CL protease of SARS- CoV 2 to overcome COVID-19 pandemic. Objectives of this study are as follow:

1. Identifying potential inhibitory compounds with therapeutic potential in essential oils of spices against 3CL protease of SARS-CoV.
2. To explore the association between a ligand and protein complex by molecular docking.
3. To determine the best interacting molecules that have inhibitory effects on the virus.

Chapter 2

Review of Literature

2.1 SARS-CoV-2

Coronaviruses (CoVs) are members of the *Coronaviridae* family (subfamily *Coronavirinae*), and the order Nidovirales. *Coronavirinae* is divided into four genera: alpha coronaviruses, beta coronaviruses, gamma coronaviruses, and delta coronaviruses [27]. Humans have been infected with the Alpha coronavirus and Beta coronavirus [28]. Coronaviruses (CoVs) are enveloped viruses with the largest known genome for an RNA virus, a single-strand, positive-sense RNA genome measuring approximately 26–32 kilo bases [29].

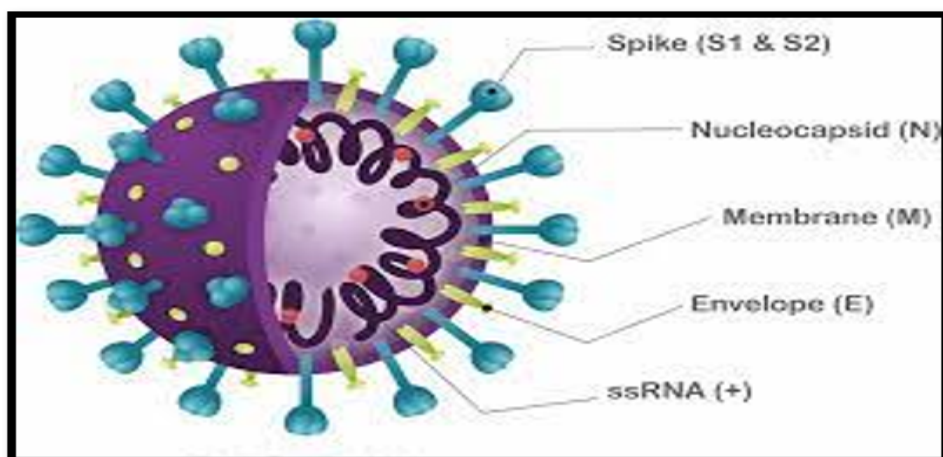


FIGURE 2.1: Structure of SARS-CoV-2 [31] .

The genomic organisation of SARS-Cov-2 is similar to that of other beta coronaviruses, with an untranslated region at the 5' end, a complex of nonstructural proteins, a spike protein gene (S), an envelope protein (E), a membrane protein (M), and a nucleocapsid protein gene (N) with untranslated regions at the 3' end. The three proteins M, E, and S are involved in the viral coat, whereas the N protein is responsible for viral genome packaging (Figure 2.1) [30] [31].

2.2 Origin

Several studies have indicated that these viruses reached the human population via intermediate hosts such as civets and camels in the case of "SARS-CoV" and "MERSCoV," respectively, from their native reservoir bats. The bat Severe Acute Respiratory Syndrome-related-Coronavirus shares 96.2% of its DNA with SARS-CoV-2 (SARSr- CoV RaTG13). The S1 subunit of pangolin CoV's spike protein was related to "SARS Cov-2" more closely than previous pandemic viruses. The genomes of the pandemic strains presently circulating were found to be 99.98-100% identical, implying a recent transfer to humans [32].

2.3 Entry and Life Cycle

The first step in the viral life cycle is virus entry into a host cell. Coronaviruses have three surface proteins: a "spike" (S), a "membrane," and a "envelope." The "M and E proteins" aid in particle assembly and discharge, while the "Spike(S) protein" binds host cell receptors and connects the viral and cellular membranes, both of which are required for infectious entry. [33], [34]. The first step in the entry of SARS-CoV-2 is the binding of S protein to the angiotensin-converting enzyme 2 (ACE2) of the host cell surface receptor [35]. Endosomal cathepsin L aids in the cleavage and activation of the virus's spike protein, allowing it to quickly fuse with the ACE2 receptor found in different human organs. The presence of the serine proteinase TMPRSS2 on the cell membrane facilitates virus entry into the

cell via direct fusion [36], [37]. Following that, the protein TMEM41B alters the shape of the ER membrane to create pockets that can serve as factories for viral replication [37], [38]. When the SARS-CoV-2 enters the cell, its genomic material is released into the cytoplasm and translated into proteins in the nucleus. Within its genome range, the virus is attained by nearly 14 Open Reading Frame (ORF), each encoding a number of proteins, both structural and non-structural, which play a role in the maintenance of the wireless power. Throughout this stage of transformation, the same gene classes that express non-structural polyproteins initially translate this process into ORF1a and ORF1b, allowing the two significant overlapping polyproteins, pp1a and pp1ab, to take part in the ribosomal frame shifting event Figure 2.2 [37].

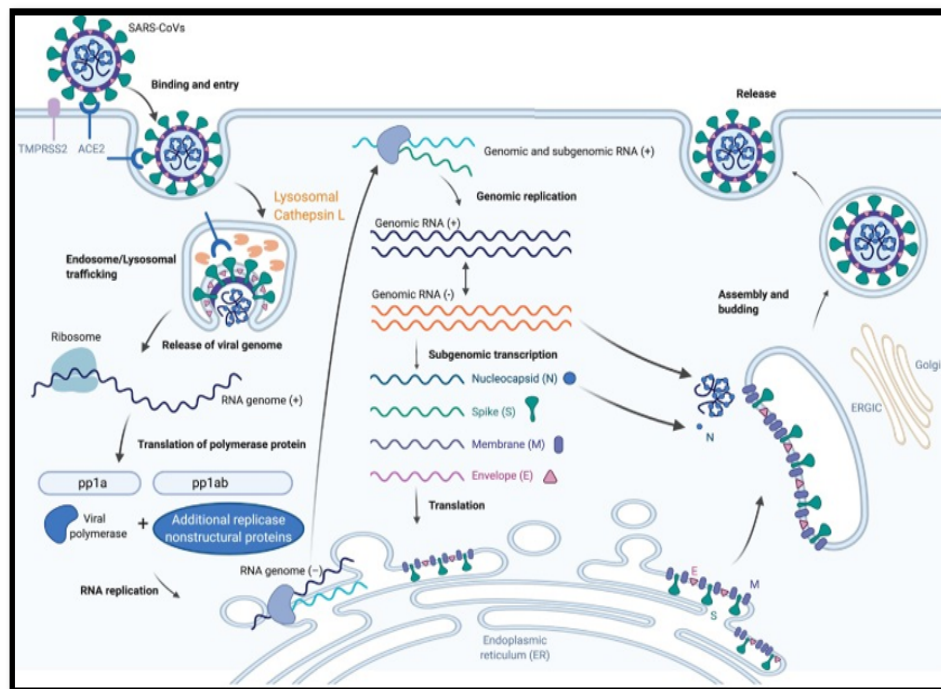


FIGURE 2.2: Severe Acute Respiratory Syndrome Coronavirus 2 (SARS-CoV-2) Lifecycle [37] .

Polyproteins are enhanced by papain-like proteases (PLpro) and serine-type Mpro (chymotrypsin-like proteases 3CLpro) encoded by nsp3 and nsp5. Numerous people with nsps form reflex transcriptase complexes (RTCs) in double membrane vesicles (DMVs), which are primarily RNA-dependent RNA polymerase (RdRp) and helicase-containing subunits [39]. The subgenomic proteins' framework and accessories are translated into peptides such as "M, S, and E," which are protected

in the "endoplasmic reticulum" before being moved to the "endoplasmic reticulum-Golgi intermediate compartment" (ERGIC). Meanwhile, the genome programme that has already been designed can encode the N protein directly in nucleocapsid form and deliver it to the ERGIC. In this chamber, nucleocapsids will join with numerous other protein molecules to form small mucous vesicles that will be exocytosed from the cell [40].

2.4 Symptoms

"COVID-19" symptoms are broad-spectrum, and disease expression can range from no signs "asymptomatic" to respiratory failure and decease. According to one study, the symptoms were temperature - 98 %, dry cough - 76 %, muscle stiffness tiredness - 44%, and mucus - 28 %, migraine - 8 %, hemoptysis - 5 %, and diarrhea - 3%.

Approximately 50 % of the patients had shortness of breath. Lymphocytopenia was found in 63% of the patients. All of the patients were suffering from pneumonia. The most serious indication was acute respiratory distress syndrome (29%) followed by acute heart injury (12%) and secondary infections (10%); 32 % needed ICU treatment [41].

2.5 Statistics

As reported by WHO at 6:03pm CET, 14 January 2022, there had been 318,648,834 confirmed cases of COVID-19, including 5,518,343 deaths worldwide. In Pakistan, from 3 January 2020 to 6:03pm CET, 14 January 2022, there had been 1,312,267 confirmed cases of COVID-19 with 28,992 deaths.

In Pakistan, 43% was the peak and rising in COVID-19 cases and there were 8 infections per 100,000 people reported. Table 2.1 shows the statistical analysis of covid-19 cases in Pakistan and globally. The total cases, recovered and death.

TABLE 2.1: Statistical analysis of Covid-19 cases in Pakistan and globally.

Statistics	Pakistan	Globally
Total Cases	1,312,267	318,648,834
Recover Cases	1,263,584	261,799,130
Deaths	28,992	5,518,343

2.6 Treatment

To the date many types of vaccines under clinical trials while 4 of them are approved, which are as follow:

1. “Viral vector vaccines”: This vaccine contains SARS-CoV-2 genetic material that is delivered by a nontoxic virus (the viral vector). When we are injected with genetic material, our cells use it to produce a specific viral protein that our immune system identifies and responds to (Figure 2.3).

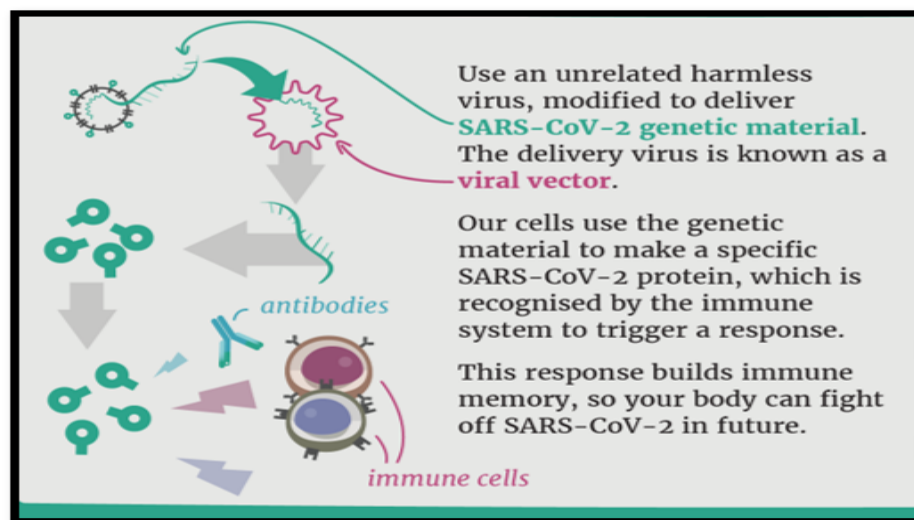


FIGURE 2.3: Viral vector vaccines [42].

This is used in the AstraZeneca to protect against COVID-19.

2. “Genetic vaccines”: The vaccines contain a genetic portion of the SARS-CoV-2 virus that causes COVID-19 to be generated. The genetic material

RNA, in the case of the "Moderna and Pfizer/BioNTech vaccines," codes for a viral protein. When we receive vaccines, our cells use the genetic material in the vaccines to produce the protein, which our immune system identifies and responds to (Figure 2.4).

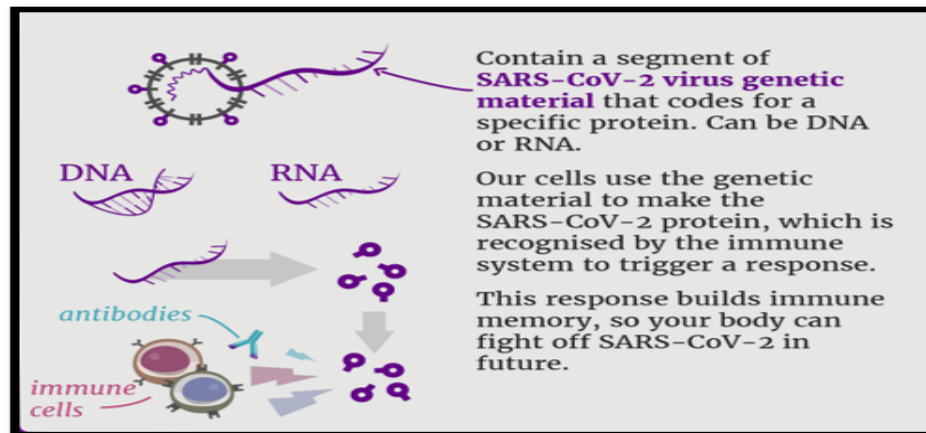


FIGURE 2.4: Genetic vaccines [42] .

3. "Inactivated vaccines": The vaccine contains a killed SARS-CoV-2 virus, which the immune system identifies and responds to without causing COVID-19 disease (Figure 2.5).

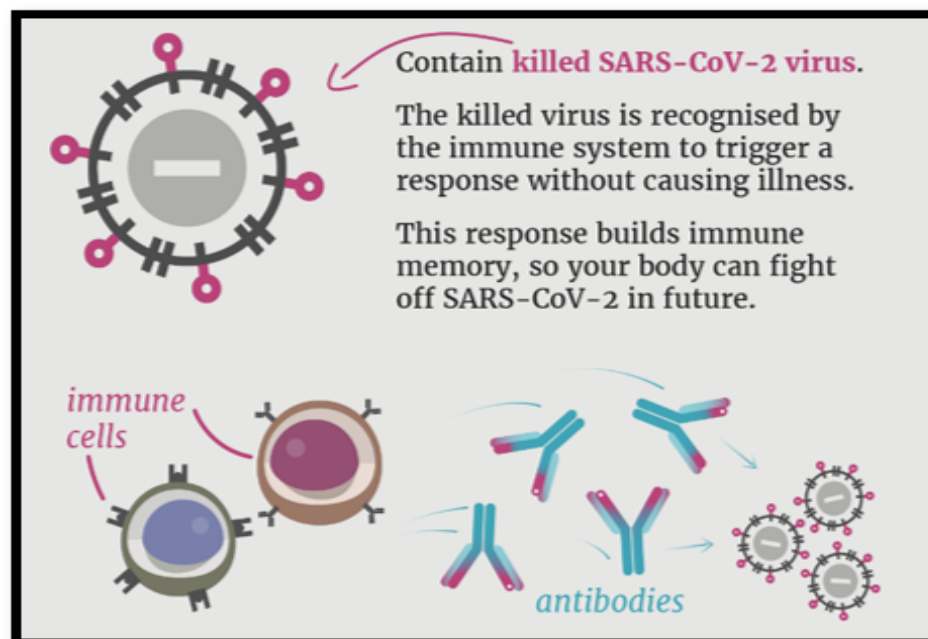


FIGURE 2.5: Inactivated vaccines [42] .

This mechanism is used by Sino vac, Sino pharm and Bharat biotech.

4. “Protein vaccines”: It is a recombinant protein subunit vaccine that specifically targets the spike protein. By attacking the spike protein, the vaccine is designed to elicit a strong immune response against the virus (Figure 2.6). Novavax is the company that developed it using the nanoparticles technique.

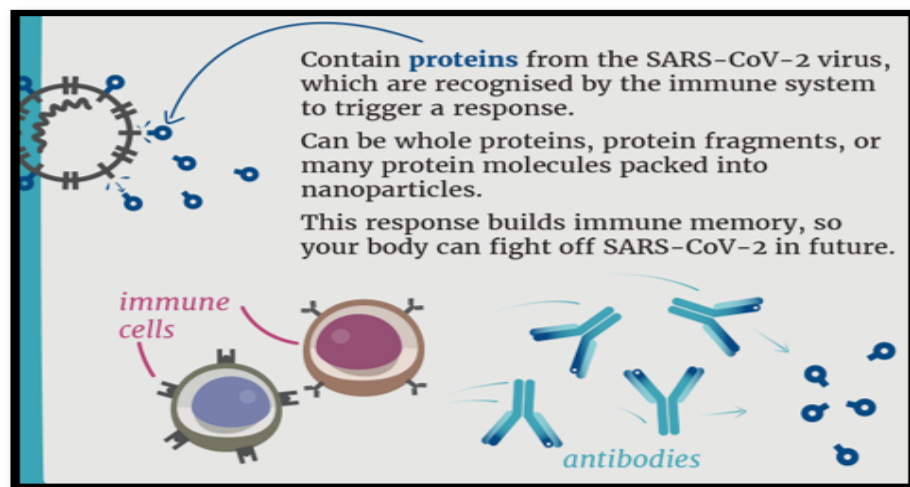


FIGURE 2.6: Protein vaccines [42].

People who had received the vaccine have also reported side effects such as pain and swelling at the injection site, tiredness, moderate to severe fever, and migraine. Dosing strategies differ depending on the type of vaccine, and symptoms may worsen with each dose phase. In the European Union, the mRNA-1273 vaccine was prescribed using a one-dose-fits-all approach, with the elderly getting a full dose and the young getting a half dose. The death rate was reduced as a result of the vaccine injection, but the complications differed from person to person [42].

2.7 Medicinal Plants

Medicinal plants are plants that have therapeutic potential or have important medicinal impacts on human or animal body. Herbal medicines have always been a significant source of bioactive substances in medical products. To treat their diseases, early humans relied on their instincts, flavours, and experience. As a

result, the history of medicinal plants is as ancient as mankind. Some plants were directly applied to injuries, while others were steamed to obtain the compounds found in the plant for treatment. Many plants' therapeutic properties have been considered for this, and these plants have played a vital role for making drugs [12].

Several hundred plant and herb species with antiviral potential had been studied. Flavonoids, terpenoids, lignans, sulphides, coumarins, saponins, furyl compounds, alkaloids, proteins, and peptides are all examples of natural substances. All of these compounds had previously been identified as active phytochemicals. Some volatile essential oils extracted from commonly used culinary herbs, spices, and herbal teas had also displayed great antiviral activity [43].

Herbal traditional medicines were used in China since the early stages of the COVID-19 outbreak. Indeed, traditional medicines helped % of the 214 patients treated rehabilitation [12], [42]. Moreover, some traditional medicinal herbs protected healthy people from SARS-CoV-2 infection and improved the patients' health with moderate or severe symptoms [12].

2.8 Essential Oils

Essential oils are volatile, natural, complex compounds with a characteristic odour that are produced by aromatic plants as secondary metabolites [45]. Plant-derived essential oils are an important component of the agricultural industry. They are frequently used as flavor enhancers in food, beverages, perfumes, pharmaceuticals, and cosmetics. Novel therapeutic molecules can be obtained from natural products and their extracts. Plant essential oils are used in a variety of industries, including medicine, agriculture, cosmetics, and food. The use of essential oils in traditional medical systems has been practiced for thousands of years in human history [46]. Essential oils have long been used for bactericidal, virucidal, fungicidal, anti-parasitic, insecticidal, cosmetic, medicinal, and cosmetic purposes, particularly in the pharmaceutical, sanitary, agricultural, and food industries [47].

2.8.1 Essential Oil of *Origanum vulgare*

The aromatic herb oregano (*Origanum vulgare*) belongs to the Lamiaceae family. *O. vulgare* is used in folk medicine to treat lung diseases, digestive disorders, menstrual cramps, osteoarthritis, scrofulosis, and urogenital disorders. It's also used in fine dining as a culinary herb [48]. In addition to its antimicrobial properties, *Origanum* has shown significant antioxidant, phytotoxic, anti-inflammatory, antifungal, and insecticidal properties in in vivo and in vitro studies [49].

Carvacrol, thymol, gamma-terpinene, and linalool are known to have high antioxidant activity and carvacrol and thymol also have antimicrobial activity against a variety of bacteria [48], [50], [53].

2.8.2 Essential Oil of *Piper nigrum*

The king of spices, black pepper (*Piper nigrum*), is one of the world's oldest and most popular spices. It is a member of the Piperaceae family and is used in many Asian countries to treat rheumatoid arthritis, digestive problems, and breathing problems⁵⁴. Beta-caryophyllene (24.24 %), limonene (16.88 %), sabinene (13.01 %), bisabolene (7.69 %), and copaene (6.3 %) are some components of essential oil [55].

2.8.3 Essential Oil of *Cinnamomum verum*

Cinnamon (*Cinnamomum verum*) is a spice derived from the bark of various trees in the genus *Cinnamomum* and the Lauracea family and is used in both sweet and savoury dishes [56]. For centuries, cinnamon has been used as a spice and in traditional herbal medicine. Cinnamon appears to have anti-inflammatory, anti bacterial, antioxidant, antitumor, cardio - vascular, cholesterol-lowering, and immunostimulatory properties [57]. The main constituents of cinnamon essential oil are (E)-cinnamaldehyde (71.50 %), linalool (7.00%), beta-caryophyllene (6.40 %), eucalyptol (5.40 %), and eugenol (4.60 %) [58]

2.8.4 Essential Oil of *Cuminum cyminum*

Cuminum cyminum is the member of Apiaceae family. Cumin oil, extracted from ripe fruit, is the plant's medicinal component. Cumin is used as a carminative in folk medicine to treat stomach disorders, diarrhoea, and colic [66], [67]. Cuminaldehyde (30.42–33.24 %), gamma-terpinen-7-al (20.54–28.36 %) [69], alpha-terpinene (6,15–12.60 %) [70], beta-cymene (4.19–5.38 %), beta-pinene (3,10–5.36 %), and p-mentha-1,4-dien-7-ol (0.71–0.99 %) were the main components in the essential oil [71], [72], [73].

2.8.5 Essential Oil of *Trachyspermum ammi*

Trachyspermum ammi is a medicinal plant in the Apiaceae family. Ajwain seeds have antimicrobial, antilithiasis, hypolipidemic, antihypertensive, antispasmodic, and diuretic properties. They are also antitussive, nematicidal, antihelminthic, and antifilarial [74], [75], [76]. Major constituents of ajwain essential oil included thymol (87.75 %), carvacrol (11.17 %), p-cymene (60.78 %), and γ -terpinene (22.26 %) [77].

2.9 Molecular Docking

Molecular docking is type of computational modelling that predicts the optimal binding orientation of one chemical molecule (a ligand) to some other chemical compound (a receptor) when the two combine to form a stable complex [78].

Molecular docking was frequently used to predict the binding arrangement of small molecules (drug candidates) to their biologically relevant target (such as protein, carbohydrate, or nucleic acid) in order to identify their binding parameters.

This provides raw data for drug discovery and development (structure-based drug development) of new agents with higher efficacy and specificity [79]. The mechanism is used by Sino vac, Sino pharm and Bharat biotech will be find.

2.10 3CL Pro or Mpro

SARS-CoV 2's viral genome encodes about 20 proteins, having two proteases (PL-pro and 3CL-pro) that are necessary for virus replication; they transform the two translated polyproteins "PP1A and PP1AB" into independent active constituents. The main protease "M pro," also known as the 3-chymotrypsin-like protease "3CL pro," has been discovered as a potential drug target [80]. 3CLpro cleaves polyproteins at eleven different locations, including a conserved Gln at the "P1" and a minor amino acid (Ser, Ala, or Gly) just before the "P1" in a process known as "auto processing," which is activated by the enzyme's own autolytic cleavage. A common characteristic was observed in many crystal structures of coronavirus 3CLpro from "TGEV, HCoV 229E, and SARS-CoV." "Residues 1-184" are two chymotrypsin-like -domains, while "Residues 201-303" is one B-helical dimerization domain. 3CLpro's active site is found in the pit between domains "I" and "II," and it comprises a catalytic pair made up of His41 and Cys145. Domain III was believed to facilitate dimer formation since the C-terminal helical domain III "residues 201-306" created a stiff dimer on their own (Figure 2.7) [81], [82].

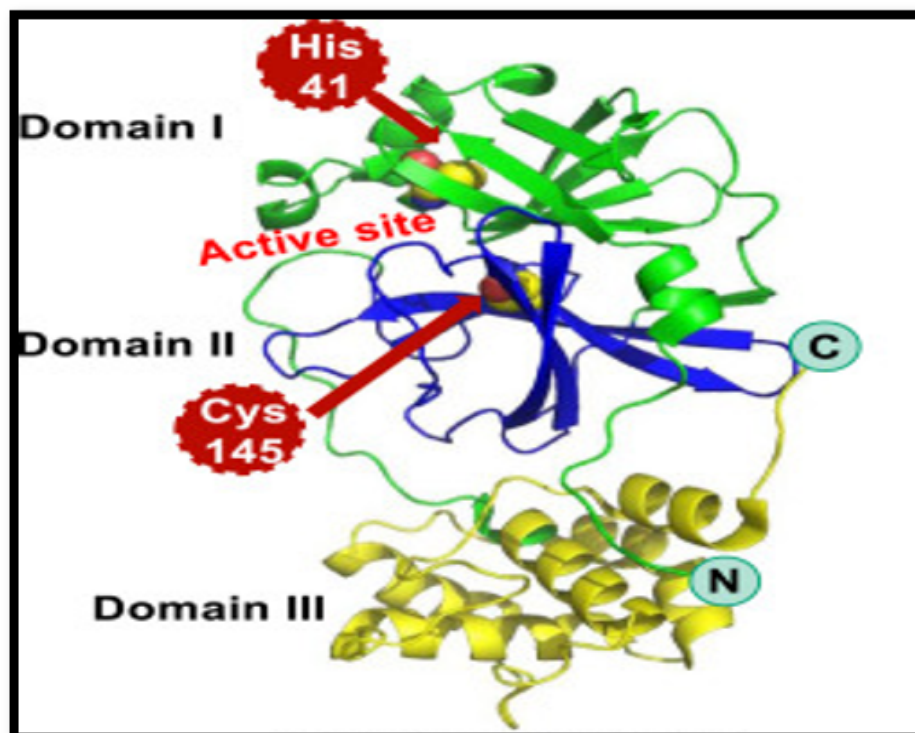


FIGURE 2.7: Structure of 3CL protease of SAES-CoV-2 [82] .

2.11 Natural Compounds as Inhibitors of 3CL Protease

Natural agents from the terpenoid and alkaloid groups suppress 3CLpro with a similar inhibitory pattern to SARS-CoV-2. The place of inhibitory activity, interaction with conserved catalytic dyad residues "Cys-145 and His-41", binding affinity and beneficial expected ADMET properties all suggest that '6-Oxoisoiguesterin,' '10-Hydroxyusambarensine,' 'Cryptoquindoline,' and '22-Hydroxyhopan-3-one' are effective against 3CL protease. To treat the viral illness, a variety of phenolic plants were often used. Indigo, indirubin, B-sitosterol, and Y-sitosterol are among the phytochemicals contained in *I. tinctoria* L. root. Seven different compounds were studied for their potential to inhibit 3CLpro, including aloe-emodin, hesperetin, quercetin, emodin, and chrysophanol. In a cell-based experiment, aloe-emodin, sinigrin, and hesperetin were found to decrease 3CLpro cleavage ability in a dose-dependent manner [82]. "Chalcones", "flavanones", and "oumarins" from *Angelicae Sinensis Radix* had dose-dependent inhibitory effects against SARS-CoV by blocking the action of 3CLpro. Furthermore, phytochemicals such as hesperetin and sinigrin isolates obtained from *Isatidis Radix*, tingenone, celastrol, pristimerin, and iguesterin isolated from *Tritergium regelii*, and quercetin derivatives quercetin-3- β -galactoside have antiviral activity against SARS-CoV by targeting SARS-CoV 3CLpro [25]. Natural agents from the alkaloids and terpenoids classes, are effective in suppressing the 3CLpro with a conserved inhibitory pattern to SARS-CoV-2. The site of inhibitory activity, binding affinity, interaction with conserved catalytic dyad residues "Cys-145 and His-41," and favourable expected ADMET parameters all point to '6-Oxoisoiguesterin,' '10-Hydroxyusambarensine,' 'Cryptoquindoline,' and '22-Hydroxyhopan-3-one' being effective against SARS-CoV-2 3CL protease [82]. Numerous phenolic herbs were commonly used to treat the viral infection. Phytochemicals found in *I. tinctoria* L. root include indigo, indirubin, indican, B-sitosterol, sinigrin, and Y-sitosterol. Seven other compounds, including aloe-emodin, daidzein, hesperetin, quercetin, naringenin, emodin, and chrysophanol, were tested for their ability to inhibit SARS-CoV 3CLpro [82].

Chapter 3

Research Methodology

3.1 Methodology Flowchart

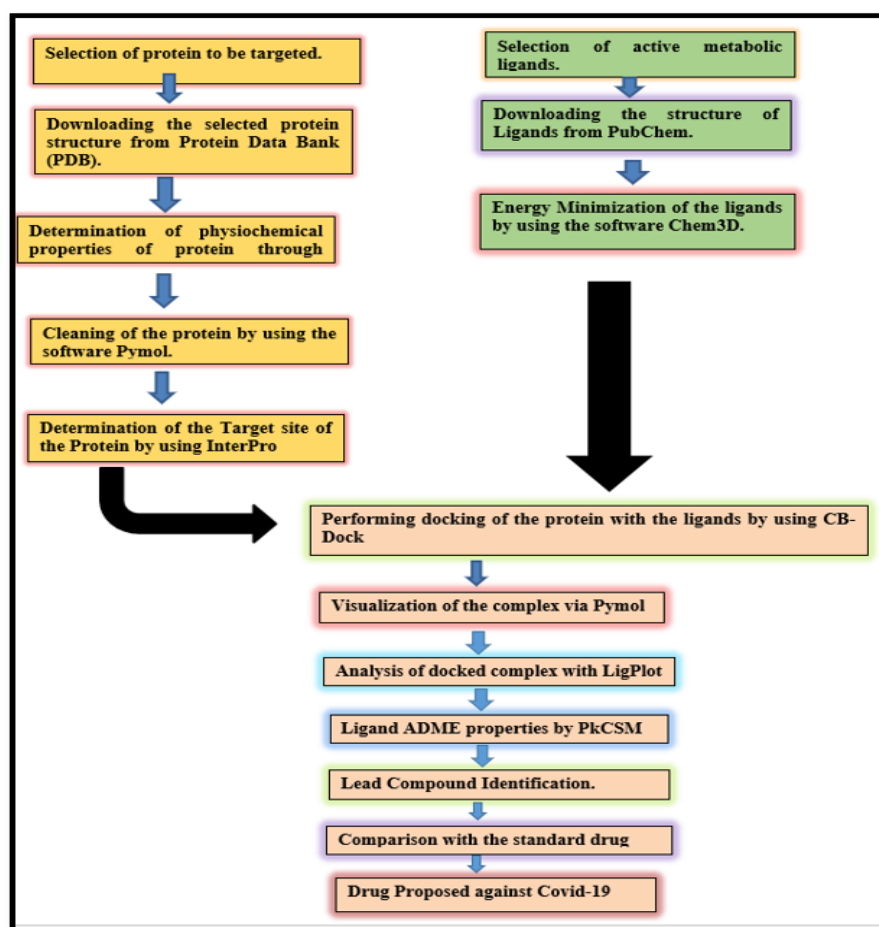


FIGURE 3.1: The flowchart of research methodology.

3.2 Selection of Disease

The unpredicted pandemic caused by the novel coronavirus 2019 (COVID-19) had caused widespread panic. COVID-19 had caused havoc, and scientists and doctors were urged to test the safety and effectiveness of drugs used to treat this illness. In such a pandemic situation, the government had taken a number of steps to prevent and control the SARS-CoV-2. Because of the pandemic situation, scientists had to rethink strategies for combating viral infections through drugs, therapies, and precautions. COVID-19 treatment involves limiting viral multiplication as well as neutralizing tissue damage caused by an inappropriate immune response. Nowadays, several COVID-19 diagnostic kits are available, and re-purposing COVID-19 medications has been shown to be effective for patients [82].

3.3 Selection of Protein

3CL-pro is required for virus replication because it converts the two polyproteins “PP1A and PP1AB” into distinct active constituents. The 3-chymotrypsin-like protease “3CL pro,” which is also called as the main protease “M pro,” has been identified as a potential therapeutic target [80]. Mpro cleavage of pp1a and pp1ab polyproteins leads to the production of functional proteins such as “RNA polymerase”, “endoribonuclease”, and “exoribonuclease”. Inhibition of the Mpro enzyme results in not only inhibition of viral development but also it boost the host’s innate immunity against CoV. Recently, the 3D crystal structure of 3CL protease obtained from one specific coronavirus (PDB ID: 6LU7) was published [76].

3.4 Determination of Physiochemical Properties of Proteins

The study and determination of a protein’s physical and chemical properties is critical in determining its function. ProtParam, an ExPASy tool, was used for

it. The molecular weight, isoelectric point, number of amino acids present, grand average of hydropathicity, instability index, and number of negatively charged (Asp+Glu) and positively charged (Arg+Lys) residues were investigated [77].

3.5 Cleaning of the Downloaded Protein

After downloading the protein structure, the extra constituents attached to the protein was removed using the open source system Pymol. The linear chain containing 1-301 amino acids was referred as the A chain, and the remaining protein constituents was eliminated [78].

3.6 Determination of Functional Domains of Target Proteins

InterPro, a database that can analyse a protein, was used to determine the domains of the target protein. It also provides information about the families, functional sites, and domains of the protein under study [79]. By inserting the main protease's FASTA sequence.

3.7 Selection of Active Metabolic Ligands

The active compounds which were present in the essential oils of spices were selected upon their antiviral, antibacterial and antioxidant properties.

3.8 Ligand Preparation

We had downloaded the 3-dimensional structure of the above-mentioned ligands from the PubChem database. PubChem is a database maintained by the National

Center for Biotechnology Information (ncbi) that contains information about chemical molecules. The information saved was associated with chemical names and molecular formulas. 3D or simple structures, their isomers, canonical similies, and information about the molecules' activities in biological assays [80]. The structure of the ligands obtained from PubChem were downloaded, and the MM2 energy of the ligands was minimized using Chem3D ultra. If the selected ligand structure was not available, our next attempt would be to download the canonical similies from PubChem, insert them in the software ChemDraw, and then repeat the energy minimization step using Chem3D ultra after obtaining the 3D structure [81]. Finally, the sdf format was chosen to save the ligand's energy-minimized structure.

3.9 Molecular Docking

CB-dock (Cavity detection guided blind docking) was used to perform molecular docking between the protein and the ligand. CB dock automatically locates docking locations. CB-Dock is a protein and ligand docking method that calculates the size and location of the bonding sites. The box size was adjusted based on the ligand, and docking was then performed. AutoDock Vina was used to dock the device. Because we were focused on cavity binding, the accuracy ratio was higher. We uploaded the 3D structure of the protein in pdb format and the 3D structure of the ligand in sdf format for docking. The end result of this docking would be five different poses of interaction. To choose the best pose, we considered the minimum vina score, which is expressed in KJ/m-1. CB -Dock displayed results in 5 different poses in an interactive 3D visualisation. The best pose was chosen based on the lowest vina score (kJ/m-1) [82].

3.10 Visualization of Docking Result Via PyMol

PyMol displayed the docked complex of ligand and protein. It is a free open source molecular visualisation tool that can generate high-quality 3D images of proteins,

small molecules, nucleic acids, and electron densities, among other things. This was capable of editing molecules, ray tracing, and creating movies. Docking poses generated by CB-Dock were visualised and saved as a molecule in.pdb format in a single file for further analysis [82].

3.11 Analysis of Docked Complex Via LigPlot

Once we had the docked complex with the lowest vina score, the complex was analysed. The complex was stored in pdb format. This analysis was carried out with the help of the software LigPlot. For the given pdb file format, schematic diagrams of protein and ligand interactions were created automatically. Hydrogen bonds and hydrophobic contacts influence these interactions. LigPlot analyses the hydrophobic and hydrogen bonding interactions. LigPlot generated a 2D representation of the protein-ligand complex using this method.

3.12 Ligand ADMET Properties

Following the analysis, the next step was to investigate the pharmacokinetic and toxicity properties. During preclinical ADMET, the drug's weak candidates were eliminated. The remaining candidates were chosen as potential anti-disease drugs. The PkCSM was used to optimise the ADMET (Absorption, Distribution, Metabolism, Excretion and Toxicity) of the human body [82].

3.13 Lead Compound Identification

After all the work was performed the next step was to find the lead compound. The lead compound was identified after applying the Lipinski rule of 5 which includes.

1. The log value of the drug-like compound must be limited to 5.

2. The molecular weight should also be lesser than 500.
3. Hydrogen bond acceptors maximum number should be 10.
4. Hydrogen bond donor's maximum number should be 5.

Once the compound fulfills these rule it was selected as our lead compound. The selected compound was our lead compound [81].

3.14 Comparison of Antiviral Drug Against COVID- 19 and Lead Compound

Remedisvir, a drug with antiviral properties against MERS, SARS-Cov, and other viruses, was chosen as a standard drug to compare to the lead compound. Remedisvir had been used against viral replication proteins and had shown effective results in places such as Rome and the United States [80].

Despite the fact that much work had been done in developing vaccines and drugs to combat Covid-19, there was still a gap in the treatment and cure of this disease. The active compounds derived from essential oils of spices that were chosen as the lead compound and show more positive results when compared to the existing drug can be the future of medicinal drug against COVID-19.

Chapter 4

Results and Discussions

4.1 Sequence Retrieval of Protein

3CL pro, the protein chosen, is a CoV enzyme that plays an important role in the virus's replication and transcription. As a result, it is regarded as an attractive enzyme of the virus to be focused. 3CL pro is a 33.8 kDa protein that digests polypeptides at nearly 11 conserved sites, making it an effective drug target [74].

The Protein Data Bank (PDB) contains a lot of information on protein-ligand complexes. The 3D structure of coronavirus's 3CL protease was obtained from the protein data bank (PDB) as 6LU7. The structure of 3CL protease which was available in PDB was shown in Figure 4.1.

> 6LU7-1—Chain A—3C-like proteinase—Severe acute respiratory syndrome coronavirus 2 (2697049)

```
SGFRKMAFPSGKVEGCMVQVTCGTTTLNGLWLDDVVYCPRHVICTSEDML
KVDTANPKTPKYKVFVRIQPGQTFSVLACYNGSPSGVYQCAMRPNFTIKGSF
LNGSCGSVGFNIDYDCVSFCYMHHMELPTGVHAGTDLEGNFYGPFVDRQTA
QAAGTDTTITVNVLAWLYAAVINGDRWFLNRFTTTLNDFNLVAMKYNYEPLT
QDHVDILGPLSAQTGIAVLDMCASLKELLQNGMNGRTILGSALLEDEFTPFDV
VRQCSGVTFQNPNYEDLLIRKSNHNFLVQAGNVQLRVIGHSMQNCVLKL
NPNYEDLLIRKSNHNFLVQAGNVQLRVIGHSMQNCVLKL [80].
```

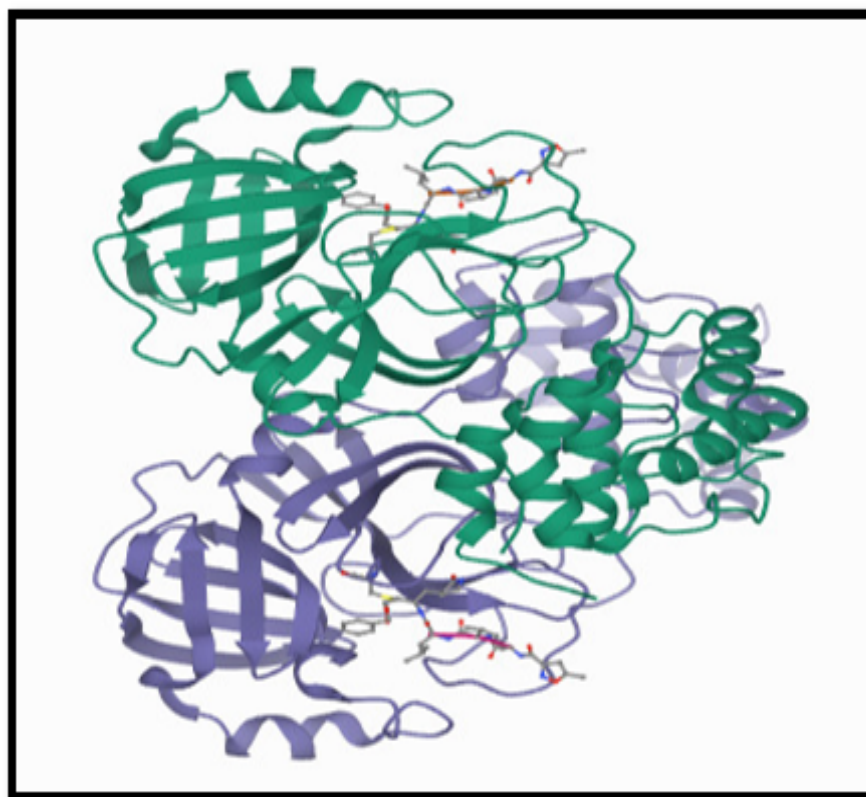


FIGURE 4.1: Structure of 3CL protease from PDB

The structure of 3CL protease which was available in PDB was shown in Figure 4.1.

4.2 Analysis of Physiochemical Properties of 3CL Protease

ProtParam, an ExPASy tool, is used to investigate the properties of protein 3CL pro. It is an online tool for determining the physical and chemical properties of proteins entered into Swiss-prot or TrEMBL databases, as well as proteins entered by users. The parameters studied include molecular weight, protein amino acid composition, atomic composition, theoretical pI, instability index, and aliphatic index [63].

A protein with a pI greater than 7 indicates that it is basic, whereas a protein with a pI less than 7 indicates that it is acidic. The aliphatic index measures a protein's

thermostability. The protein's molecular weight (MW) reveals both positive and negative amino acid residues. The negative charge residues (Asp+Glu) are denoted by NR, while the positive charge residues (Arg+Lys) are denoted by PR.

Analysis of physicochemical parameters revealed that the 3CLpro polypeptide is 306 amino-acid long with a molecular weight of 33,796.64 da, which gives the protein a stable, hydrophilic molecule capable of forming hydrogen bonds Table 4.1.

TABLE 4.1: Physiochemical properties of 3CL protease.

MW	pI	NR	PR
33796.64	5.95	26	22
Instability Index	Aliphatic Index	Amino Acids	Total Atoms
27.65	82.12	306	4686

The above table shows the molecular weight of Mpro as 33796.64 which is a collective weight of negative (NR) and positive amino acids residues (PR). The pI of the selected protein is 5.95, indicating that it is acidic in nature. The selected protein 3CLpro has a high stability index of 27.65, indicating that it is a very stable protein. The aliphatic index also indicates that the protein is thermostable.

4.3 Identification of Functional Domains

The InterPro consortium is used to identify functional domains. InterPro aids in the functional analysis of proteins and categorises them into families by locating functional domains and other important sites. Functional domains are the active parts of proteins that allow them to interact with other proteins or substances. In the case of 3CL protease of SARS-CoV-2 domains I, II and III consist of residues 1-8 and 8-184 and 201-306, respectively [63].

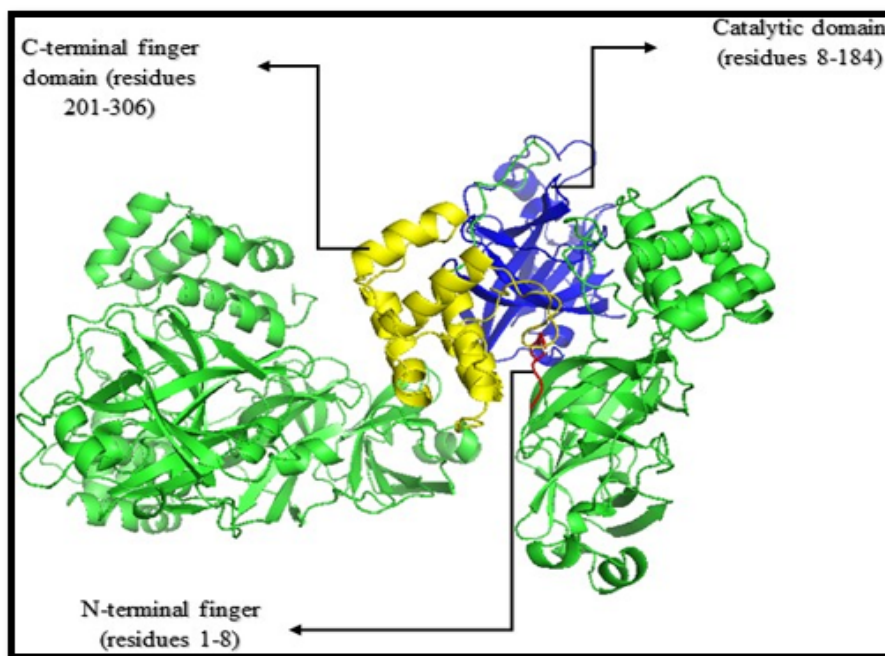


FIGURE 4.2: Functional Domains of 3CL Protease [63]

4.4 Structure of Protein Cleaned for Docking

PyMol was used to refine the selected protein before it was used in molecular docking. The extra side-chain C is also removed as shown in Figure 4.3, now the protein is ready for docking. Domains I and II are made up of antiparallel β -barrels, whereas Domain III is made up of a globular cluster composed of five antiparallel α -helices. Domain III is linked to Domain II by a 185-200 residue long loop region. Refined 3D structure of 3CL protease was shown in Figure 4.3.

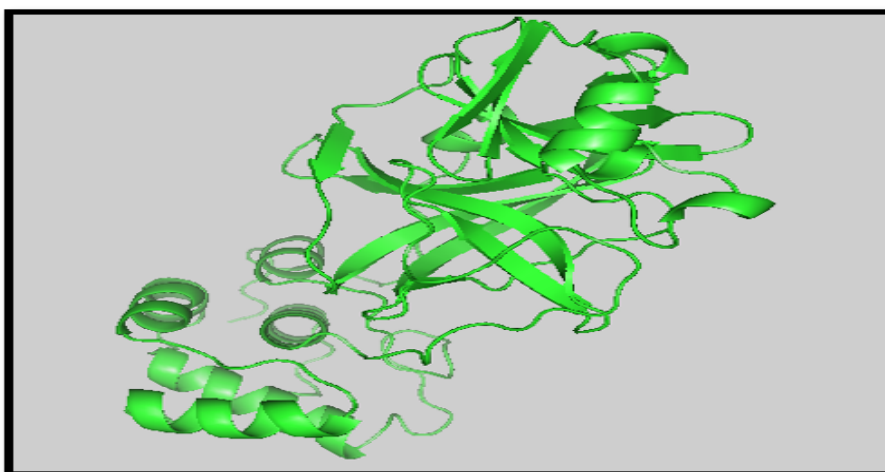


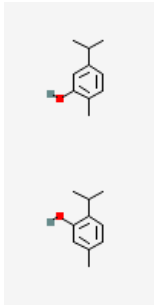
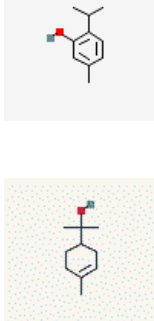
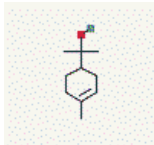
FIGURE 4.3: Refined Structure of 3CLpro for Docking.

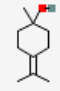
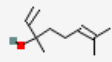
4.5 Ligand Selection

The discovery of the 3CLpro structure in SARS-CoV-2 gives the possibility to identify possible drug targets for COVID-19 treatment. Because the viral 3CLpro controls coronavirus replication and is required for its life cycle, it had been identified as a drug discovery target for SARS-CoV-2 [76]. The ligands were chosen based on their binding affinities and the best resolution structure based on the chemical class of the crystal bound to the protein. The active compounds of the selected plants' ligands were found using PubChem, the world's largest chemical databank. These ligands' 3D structures were downloaded in SDF format from PubChem and we used ChemD for energy minimization of these compounds. This is an important step because we can't just use the downloaded structure because the ligands are unstable and can affect the docking vina scores. Tables 4.2 to 4.6 showed the selected ligands from different spices.

The table 4.2 below showed molecular formula, molecular weight and structure of ligands selected from *Origanum vulgare*.



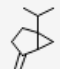
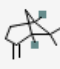
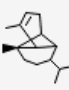
TABLE 4.2: Ligands from *Origanum vulgare*

Compounds	Molecular Formula	Molecular Weight (g/mol)	Structure
Carvacrol	C ₁₀ H ₁₄ O	150.22	
Thymol	C ₁₀ H ₁₄ O	150.22	
Alpha-terpineol	C ₁₀ H ₁₈ O	154.25	

Gamma-terpineol	$C_{10}H_{18}O$	154.25	
Linalool	$C_{10}H_{18}O$	154.25	

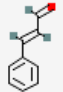
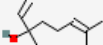

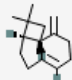
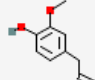
The table 4.3 below showed molecular formula, molecular weight and structure of ligands selected from *Piper nigrum*.

TABLE 4.3: Ligands from *Piper nigrum*

Compounds	Molecular Formula	Molecular Weight (g/mol)	Structure
Beta caryophyllene	$C_{15}H_{24}$	204.35	
Piperine	$C_{17}H_{19}NO_3$	285.34	
Sabinene	$C_{10}H_{16}$	136.23	
Beta-pinene	$C_{10}H_{16}$	204.35	
Alpha-copaene	$C_{15}H_{24}$	220.35	

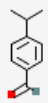
The table 4.4 below showed molecular formula, molecular weight and structure of ligands selected from *Cinnamomum verum*.

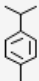
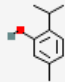
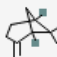
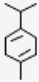
TABLE 4.4: Ligands from *Cinnamomum verum*

Compounds	Molecular Formula	Molecular Weight (g/mol)	Structure
Cinnamaldehyde	C ₉ H ₈ O	132.16	
Linalool	C ₁₀ H ₁₈ O	154.25	
Eucalyptol	C ₁₀ H ₁₈ O	154.25	
Beta-caryophyllene	C ₁₅ H ₂₄	204.35	
Eugenol	C ₁₀ H ₁₂ O ₂	164.20	

The table 4.5 below showed molecular formula, molecular weight and structure of ligands selected from *Cuminum cyminum*.

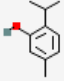
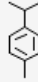
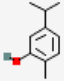
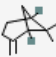
TABLE 4.5: Ligands from *Cuminum cyminum*

Compounds	Molecular Formula	Molecular Weight (g/mol)	Structure
Cinnamaldehyde	C ₁₀ H ₁₂ O	148.20	

P-Cymene	$\text{CH}_3\text{C}_6\text{H}_4\text{CH}(\text{CH})_2$	134.22	
Thymol	$\text{C}_{10}\text{H}_{14}\text{O}$	150.22	
Beta-pinene	$\text{C}_{10}\text{H}_{16}$	136.23	
Gamma-Terpinene	$\text{C}_{10}\text{H}_{16}$	136.23	

The table 4.6 below showed molecular formula, molecular weight and structure of ligands selected from *Trachyspermum ammi*.

TABLE 4.6: Ligands from *Trachyspermum ammi*

Compounds	Molecular Formula	Molecular Weight (g/mol)	Structure
Thymol	$\text{C}_{10}\text{H}_{14}\text{O}$	150.22	
P-cymene	$\text{CH}_3\text{C}_6\text{H}_4\text{CH}$	134.22	
Carvacrol	$\text{C}_{10}\text{H}_{14}\text{O}$	150.22	
Beta-pinene	$\text{C}_{10}\text{H}_{16}$	136.23	

Terpinene-4-ol $C_{10}H_{18}O$ 154.25

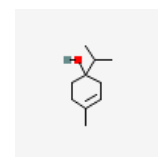


Table showed the physiochemical properties of different ligands selected from 5 different spices. Physiochemical properties includes molecular weight, molecular formula and structure. All the selected ligands showed good physiochemical properties.

4.6 Virtual Screening

The most important issue during drug development is safety, which includes a variety of toxicities and unfavorable drug effects that should be evaluated in the preclinical and clinical phases [76]. Selected ligands from the PubChem database follow the Lipinski rule, as shown in Table 4.7. The log p value of the molecule should be limited to 5, the molecular weight should be less than 500, the maximum number of H bond acceptors should be 10, and the maximum number of H bond donors should be 5.

TABLE 4.7: Selected ligands showing Lipinski rule of five.

Ligands	Log P Value	Molecular Weight	HBD	HBA	Rotatable Bonds
Carvacrol	2.82402	150.22	1	1	1
Thymol	2.82402	150.22	1	1	1
Alpha-terpineol	2.5037	154.25	1	1	1
Gamma-terpineol	2.6478	154.25	1	1	0
Linalool	2.6698	154.25	1	1	4

TABLE 4.7: Selected ligands showing Lipinski rule of five.

Ligands	Log P Value	Molecular Weight	HBD	HBA	Rotatable Bonds
Beta-caryophyllene	4.7252	204.35	0	0	0
Piperine	2.9972	285.34	3	0	3
Sabinene	2.9987	136.23	0	0	1
Beta-pinene	2.9987	136.23	0	0	0
Alpha-copaene	4.2709	204.35	0	0	1
Cinnamaldehyde	1.8987	132.16	1	0	2
Linalool	2.6698	154.25	1	1	4
Beta-caryophyllene	4.7252	204.35	0	0	0
Eucalyptol	2.7441	154.25	1	0	0
Eugenol	2.1293	164.20	2	1	3
Cumin-aldehyde	2.6225	148.20	1	0	2
P-Cymene	3.11842	134.22	0	0	1
Beta-pinene	2.9987	136.23	0	0	0
Gamma-terpinene	3.3089	136.23	0	0	1
Thymol	2.82402	150.22	1	1	1
Thymol	2.82402	150.22	1	1	1

TABLE 4.7: Selected ligands showing Lipinski rule of five.

Ligands	Log P Value	Molecular Weight	HBD	HBA	Rotatable Bonds
Carvacrol	2.82402	150.22	1	1	1
P-cymene	3.11842	134.22	0	0	1
Beta-pinene	2.9987	136.23	0	0	0
Terpinene-4-ol	2.5037	154.25	1	1	1

Table showed 4.7 that all the ligands had followed Lipinski rule of five. It includes molecular weight, log P value, hydrogen bond acceptor (HBA), hydrogen bond donor (HBD) and rotatable bonds. Gamma-terpineol had log p value 2.6478 with molecular weight of 154.25 g/mol. Piperine had log P value of 2.9972 and molecular weight was 285.34 g/mol. Cinnamaldehyde had log P value of 1.8987 while the molecular weight was 132.16 g/mol. Cuminaldehyde had log P value of 2.6225 with molecular weight of 148.20 g/mol and Terpinene-4-ol had shown log P value of 2.5037 while molecular weight was 154.25 g/mol.

4.7 Molecular Docking

Molecular docking is a technique that uses the vina score function to estimate the strength of a ligand bonded to a receptor protein and to determine the correct structure of the ligand that binds to the binding site. Docking was performed using the 3D structures of the ligands and the protein. CB dock, an online blind auto docking tool was used for this purpose. The receptor protein 3CL pro and the 25 ligands selected above were used in molecular docking.

The protein was in PDB format, and the ligands were in SDF. CB dock then validates the input files before converting them to pdb format. Then CB dock predicts the receptor's cavities and calculates the centres and sizes of the top

five cavities. The best of the five best conformations is chosen based on a high affinity score of the interaction between both the protein and the ligand. CB-Dock presented results in 5 different poses in an interactive 3D visualisation. The best pose was chosen based on the lowest vina score (kJ/m-1) [77].

Protein-ligand docking is an effective technique for computer-aided drug discovery (CADD) [78]. Tables 4.8 displays the ligands with the highest binding scores.

TABLE 4.8: Docking results of selected ligands.

Ligands	Binding Score (kJ/m-1)	Cavity Size	Log P Value	Molecular Weight	HBD	HBA	Rotatable Bonds
Carvacrol	-5.3	212	2.82 402	150.22	1	1	1
Thymol	-5	548	2.82 402	150.22	1	1	1
Alpha-terpineol	-5.3	548	2.50 37	154.25	1	1	1
Gamma-terpineol	-5.2	212	2.64 78	154.25	1	1	0
Linalool	-4.9	258	2.66 98	154.25	1	1	4
Beta-caryophyllene	-5.9	212	4.72 52	204.35	0	0	0
Piperine	-7	688	2.99 72	285.34	3	0	3
Sabinene	-5	212	2.99 87	136.23	0	0	1
Beta-pinene	-4.7	212	2.99 87	136.23	0	0	0

TABLE 4.8: Docking results of selected ligands.

Ligands	Binding Score (kJ/m-1)	Cavity Size	Log P Value	Molecular Weight	HBD	HBA	Rotatable Bonds
Alpha-copaene	-6	212	4.2709	204.35	0	0	1
Cinnamaldehyde	-5.2	212	1.8987	132.16	1	0	2
Linalool	-4.9	258	2.6698	154.25	1	1	4
Beta-caryophyllene	-5.9	212	4.7252	204.35	0	0	0
Eucalyptol	-5.1	212	2.7441	154.25	1	0	0
Eugenol	-5.5	212	2.1293	164.20	2	1	3
Cuminaldehyde	-5.2	212	2.6225	148.20	1	0	2
P-Cymene	-5.1	212	3.1184	134.22	0	0	1
Beta-pinene	-4.7	212	2.9987	136.23	0	0	0
Gamma-terpinene	-5.1	212	3.3089	136.23	0	0	1
Thymol	-5	548	2.8240	150.22	1	1	1
Thymol	-5	548	2.8240	150.22	1	1	1
Carvacrol	-5.3	212	2.8240	150.22	1	1	1

TABLE 4.8: Docking results of selected ligands.

Ligands	Binding Score (kJ/m-1)	Cavity Size	Log P Value	Molecular Weight	HBD	HBA	Rotatable Bonds
P-cymene	-5.1	212	3.11 842	134.22	0	0	1
Beta-pinene	-4.7	212	2.99 87	136.23	0	0	0
Terpinene-4-ol	-4.7	212	2.50 37	154.25	1	1	1

Table showed 4.8 the docking results of selected ligands. Gamma-terpineol showed binding score of -5.2 kJ/m-1 and cavity size was 212. Piperine showed binding score of -7 kJ/m-1 and cavity size was 688. Cinnamaldehyde had shown binding score -5.2 kJ/m-1 with cavity size of 212. Cuminaldehyde showed binding score -5.2 kJ/m-1 and cavity size was 212 and Terpinene-4-ol had shown binding score of -4.7 with cavity size of 212.

4.8 Interaction of Ligands and Targeted Protein

In computational biology, LigPlot generates a schematic 2D representation of a protein-ligand complex, allowing for the rapid inspection of many enzyme complexes and demonstrating a simple and informative representation of the intermolecular interactions and their strengths, including hydrogen bonds, hydrophobic interactions, and atom accessibility [79].

LigPlot was used to analyse the docked complex (pdb), which automatically generates schematic diagrams of protein-ligand interactions for a given PDB file [80]. 2D representation of docked complexes were shown in Figures 4.4 – 4.28.

Figure 4.4 showed the interaction of carvacrol with 3CL protease. It showed that carvacrol had formed three hydrogen bonds but no hydrophobic interaction.

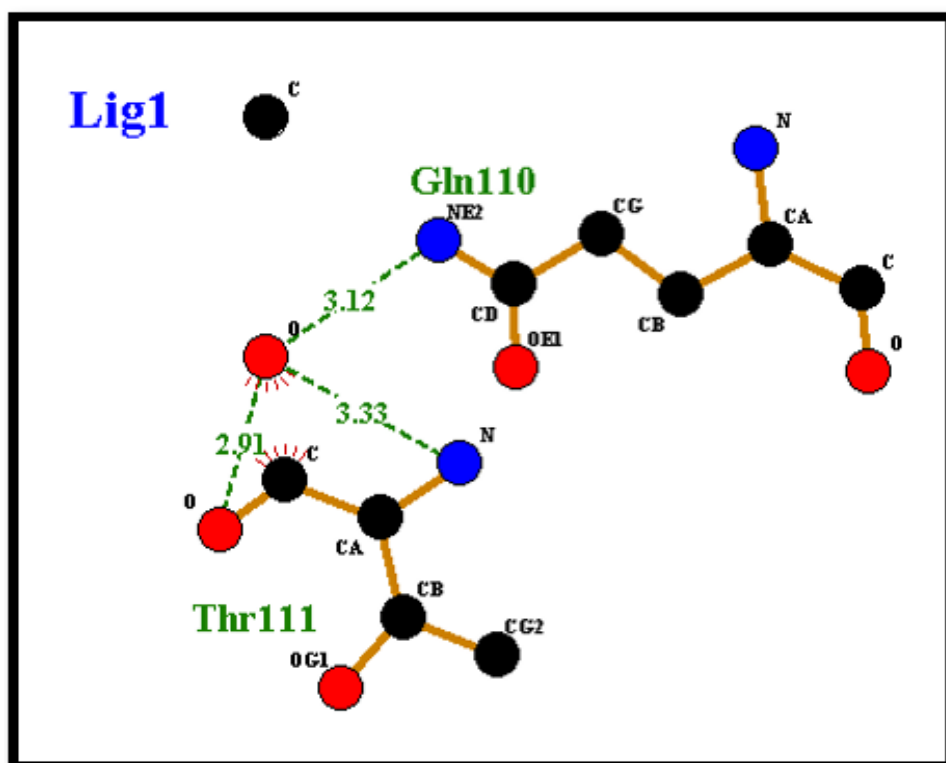


FIGURE 4.4: 2D structure showing interaction of Carvacrol with 3CL pro.

Figure 4.5 showed the interaction of thymol with 3CL protease. It showed that thymol had formed two hydrophobic interactions and two hydrogen bonds.

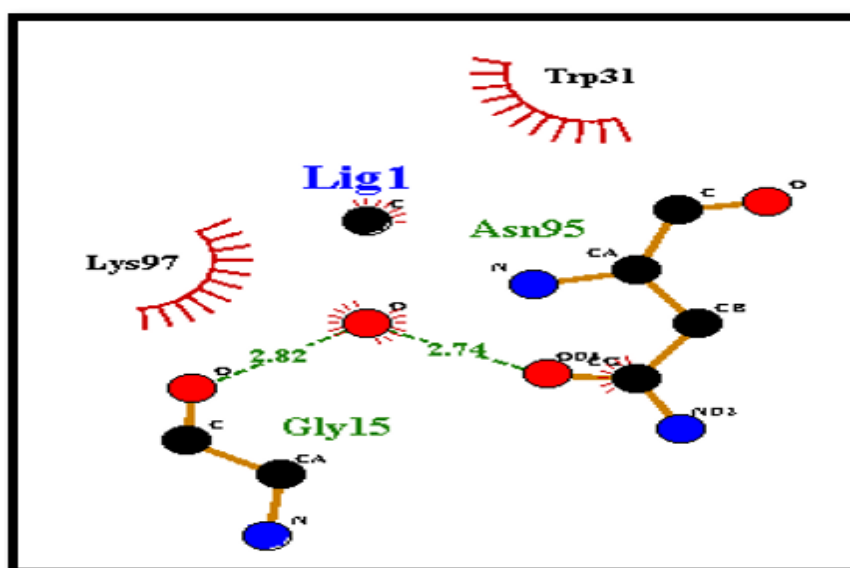


FIGURE 4.5: 2D structure showing interaction of Thymol with 3CL pro.

Figure 4.6 showed the interaction of alpha-terpineol with 3 CL protease. It showed that alpha-terpineol had formed two hydrophobic interactions and two hydrogen bonds.

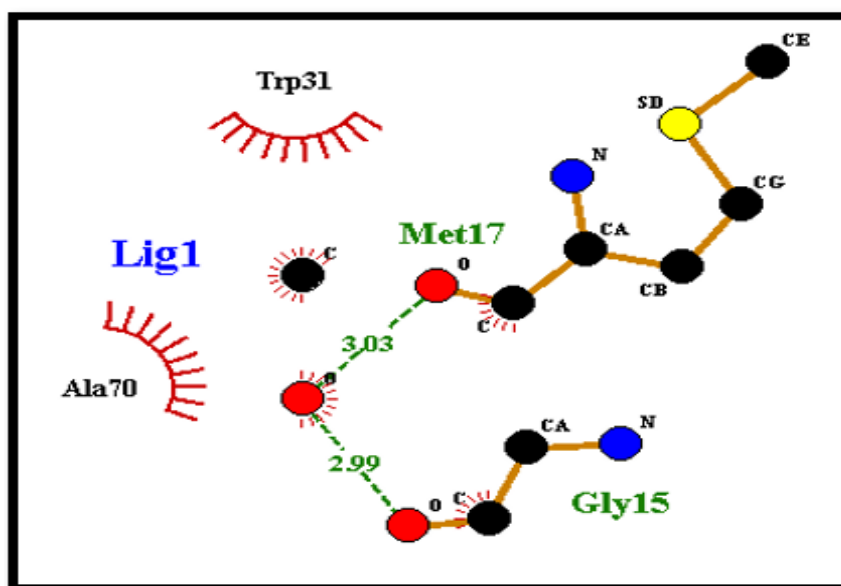


FIGURE 4.6: 2D structure showing interaction of Alpha-terpineol with 3CL pro.

Figure 4.7 showed the interaction of gamma-terpineol with 3 CL protease. It showed that gamma-terpineol had formed two hydrophobic interactions and two hydrogen bonds.

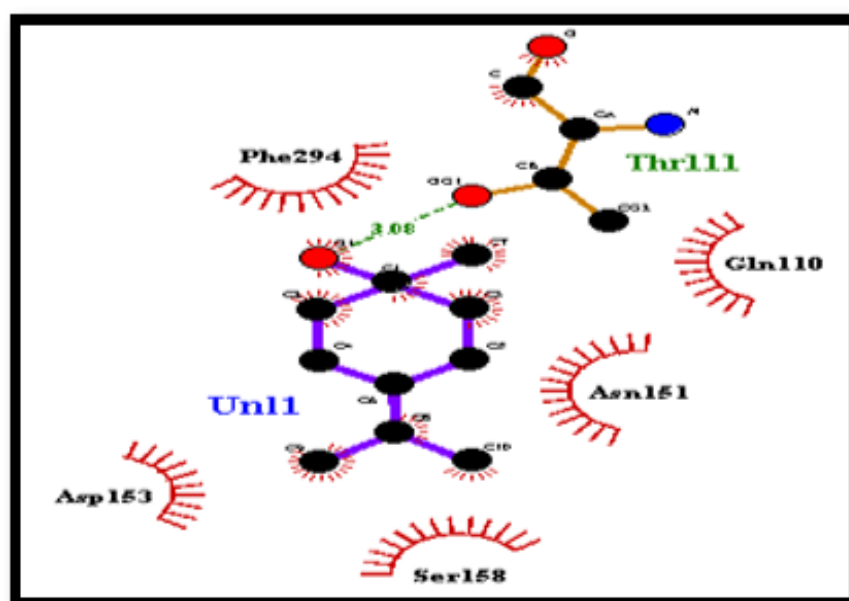


FIGURE 4.7: 2D structure showing interaction of Gamma-terpineol with 3CL pro.

Figure 4.8 showed the interaction of linalool with 3 CL protease. It showed that linalool had formed one hydrophobic interaction and one hydrogen bond.

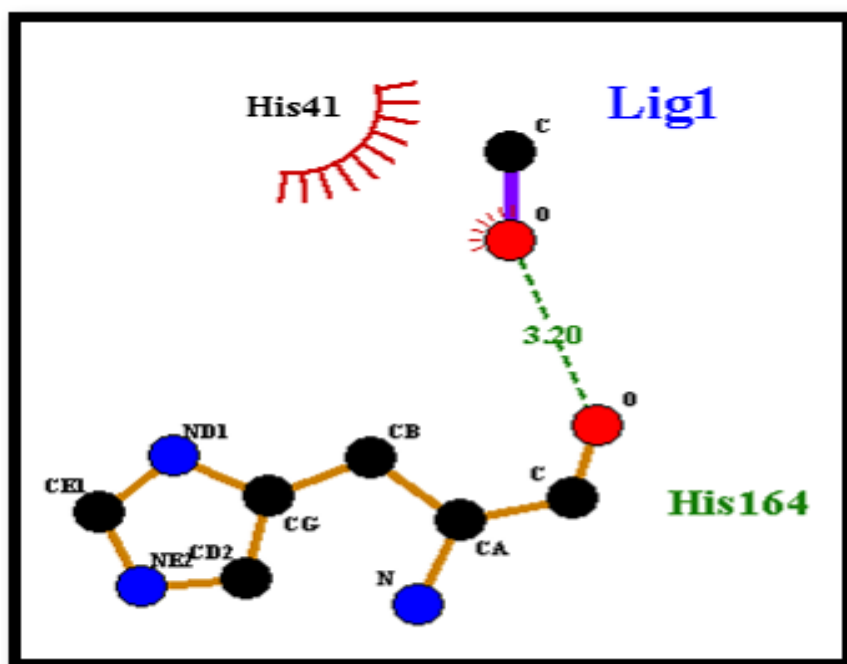


FIGURE 4.8: 2D structure showing interaction of Linalool with 3CL pro.

Figure 4.9 showed the interaction of beta-caryophyllene with 3 CL protease. It showed that beta-caryophyllene had formed nine hydrophobic interaction but no hydrogen bond.

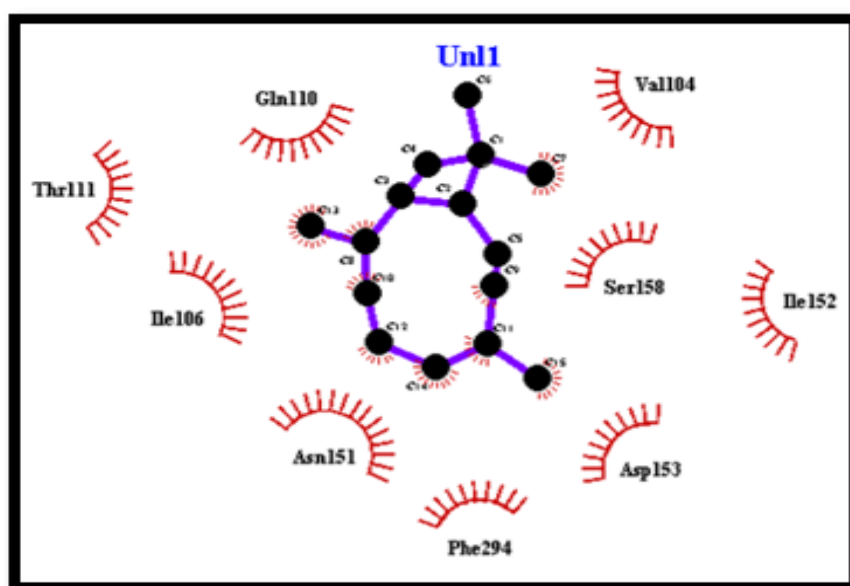


FIGURE 4.9: 2D structure showing interaction of Beta-caryophyllene with 3CL pro.

Figure 4.10 showed the interaction of piperine with 3 CL protease. It showed that piperine had formed seven hydrophobic interaction and two hydrogen bond.

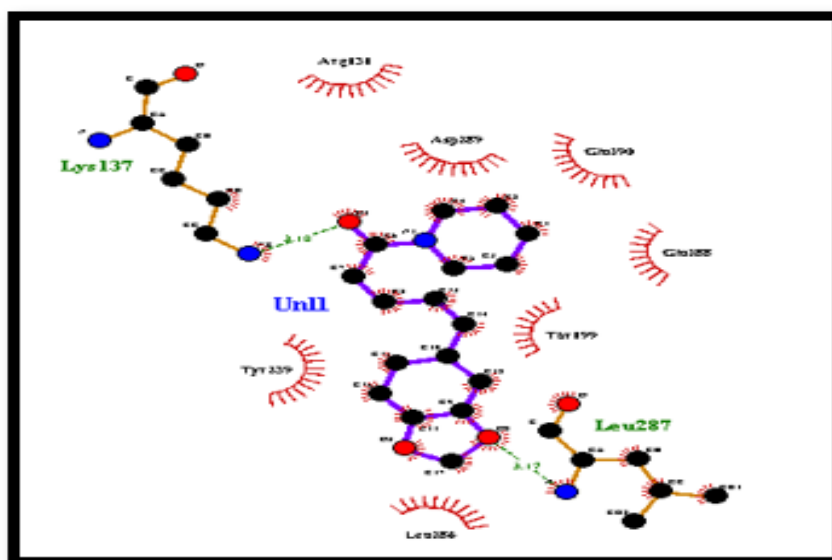


FIGURE 4.10: 2D structure showing interaction of Piperine with 3CL pro.

Figure 4.11 showed the interaction of sabinene with 3 CL protease. It showed that sabinene had neither formed hydrophobic interaction nor hydrogen bond.

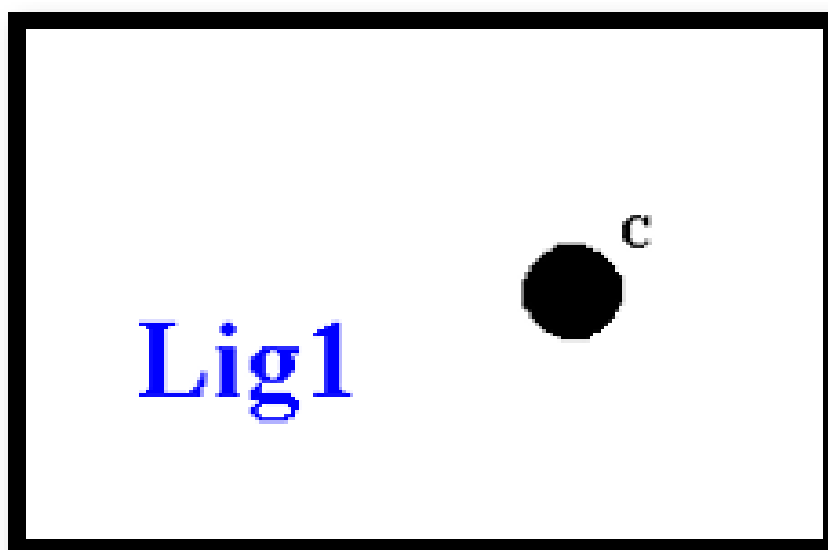


FIGURE 4.11: 2D structure showing interaction of Sabinene with 3CL pro.

Figure 4.12 showed the interaction of beta-pinene with 3 CL protease. It showed that beta-pinene had formed five hydrophobic interaction but no hydrogen bond.

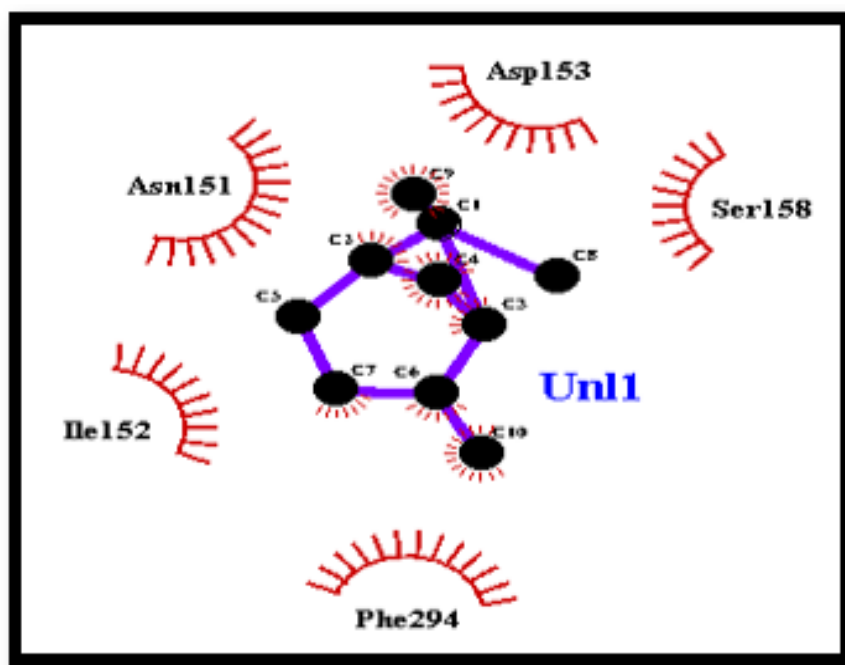


FIGURE 4.12: 2D structure showing interaction of Beta-pinene with 3CL pro.

Figure 4.13 showed the interaction of alpha-copaene with 3 CL protease. It showed that alpha-copaene had formed one hydrophobic interaction but no hydrogen bond.

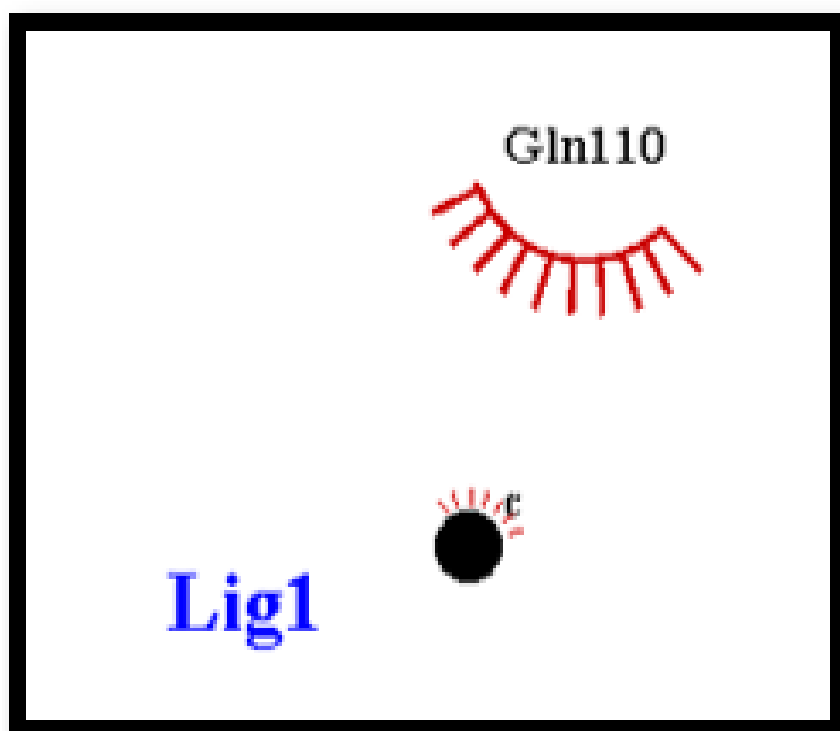


FIGURE 4.13: 2D structure showing interaction of Alpha-copaene with 3CL pro.

Figure 4.14 showed the interaction of cinnamaldehyde with 3 CL protease. It showed that cinnamaldehyde had formed four hydrophobic interaction and three hydrogen bond.

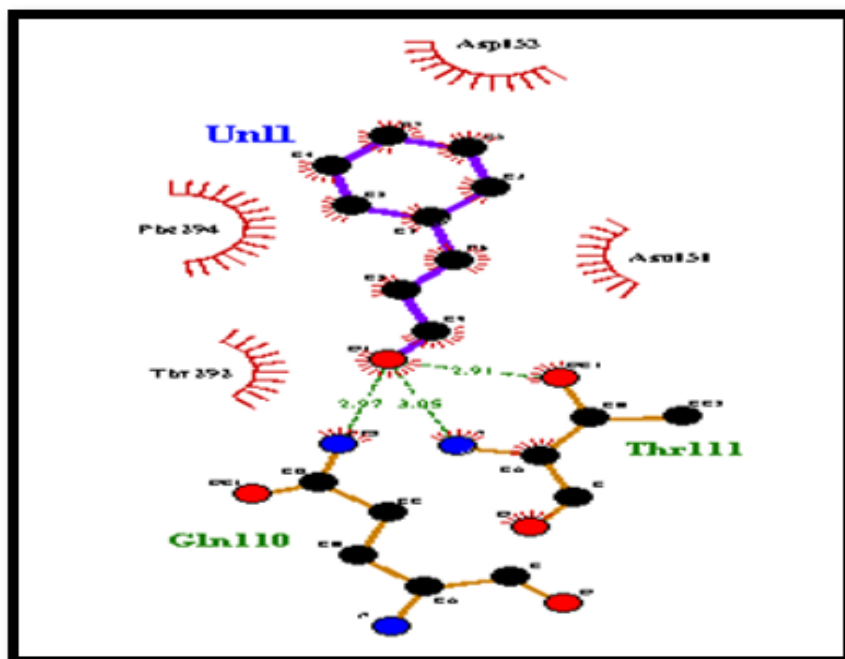


FIGURE 4.14: 2D structure showing interaction of Cinnamaldehyde with 3CL pro.

Figure 4.15 showed the interaction of linalool with 3 CL protease. It showed that linalool had formed one hydrophobic interaction and one hydrogen bond.

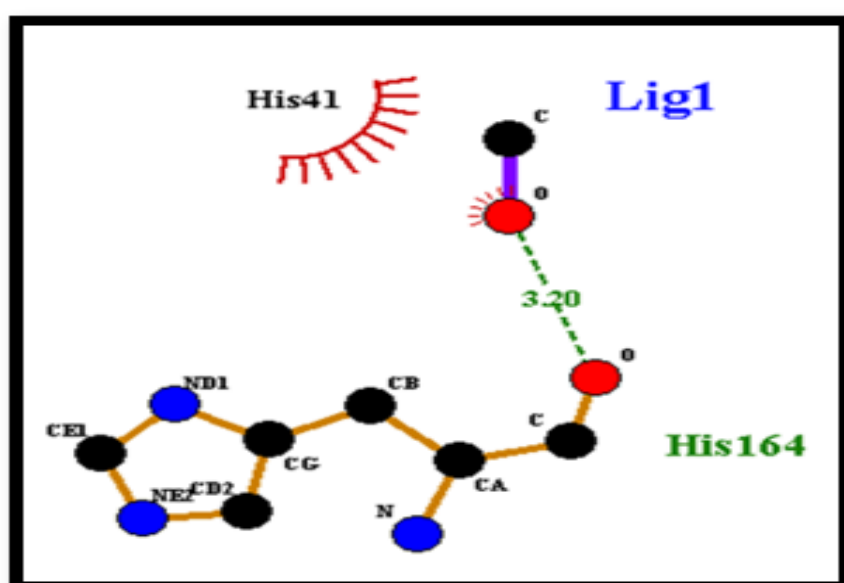


FIGURE 4.15: 2D structure showing interaction of Linalool with 3CL pro.

Figure 4.16 showed the interaction of beta-caryophyllene with 3 CL protease. It showed that beta-caryophyllene had formed nine hydrophobic interaction but no hydrogen bond.

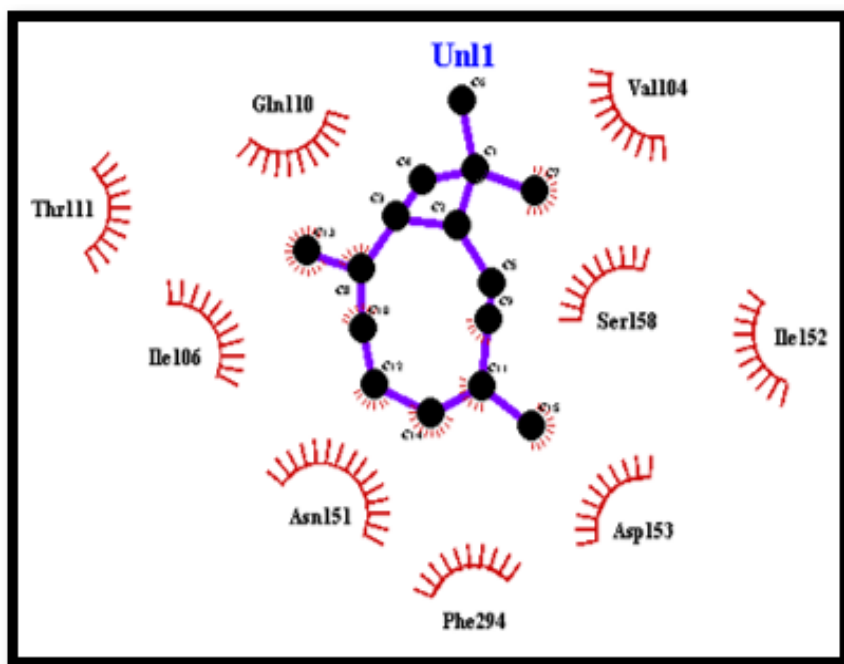


FIGURE 4.16: 2D structure showing interaction of Beta-caryophyllene with 3CL pro.

Figure 4.17 showed the interaction of eucalyptol with 3 CL protease. It showed that eucalyptol had formed six hydrophobic interaction but no hydrogen bond.

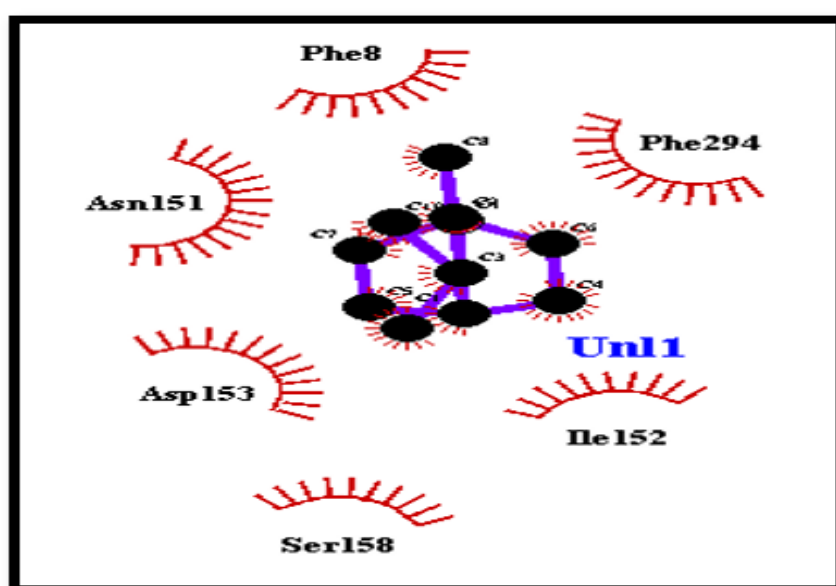


FIGURE 4.17: 2D structure showing interaction of Eucalyptol with 3CL pro.

Figure 4.18 showed the interaction of eugenol with 3 CL protease. It showed that eugenol had formed one hydrophobic interaction and one hydrogen bond.

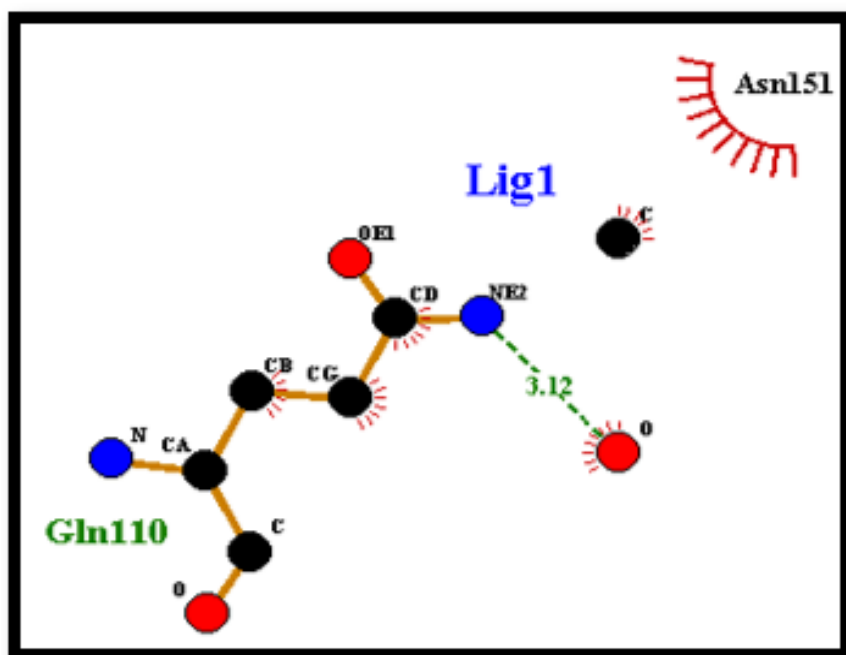


FIGURE 4.18: 2D structure showing interaction of Eugenol with 3CL pro.

Figure 4.19 showed the interaction of cuminaldehyde with 3 CL protease. It showed that cuminaldehyde had formed six hydrophobic interaction and two hydrogen bond.

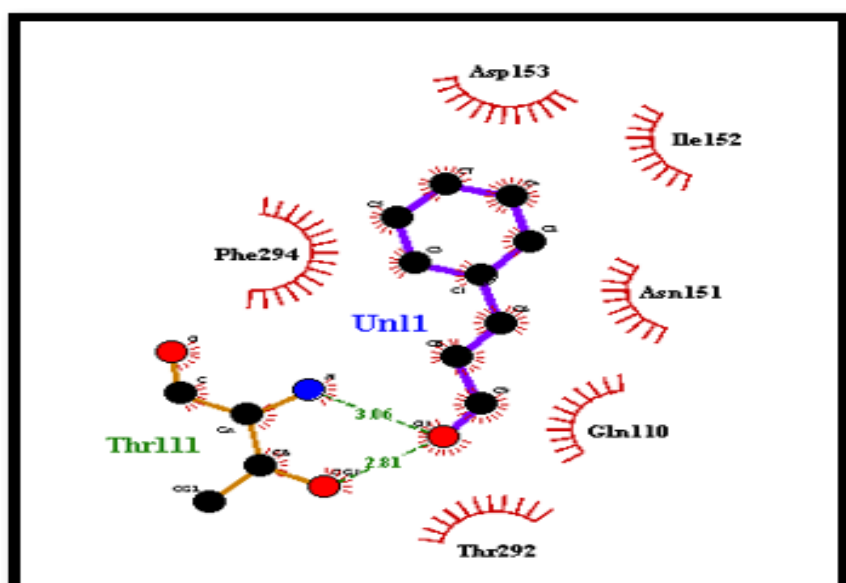


FIGURE 4.19: 2D structure showing interaction of Cuminaldehyde with 3CL pro.

Figure 4.20 showed the interaction of p-cymene with 3 CL protease. It showed that p-cymene had formed one hydrophobic interaction but no hydrogen bond.

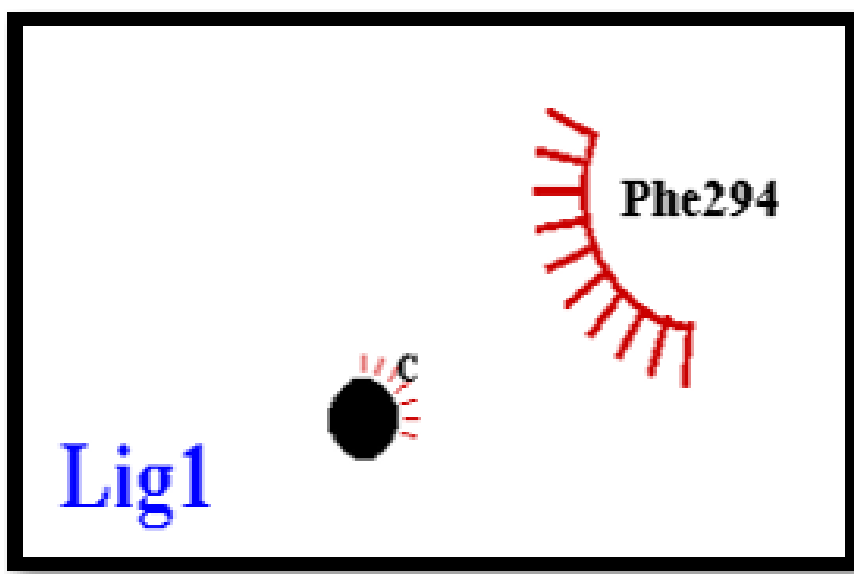


FIGURE 4.20: 2D structure showing interaction of P-cymene with 3CL pro.

Figure 4.21 showed the interaction of gamma-terpinene with 3 CL protease. It showed that gamma-terpinene had formed one hydrophobic interaction but no hydrogen bond.

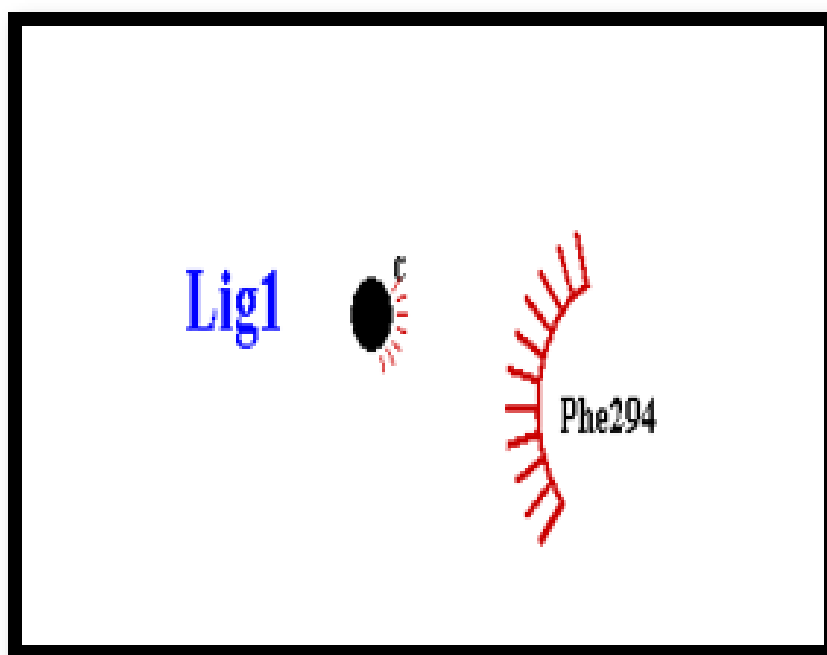


FIGURE 4.21: 2D structure showing interaction of Gamma-terpinene with 3CL pro.

Figure 4.22 showed the interaction of beta-pinene with 3 CL protease. It showed that beta-pinene had formed five hydrophobic interaction but no hydrogen bond.

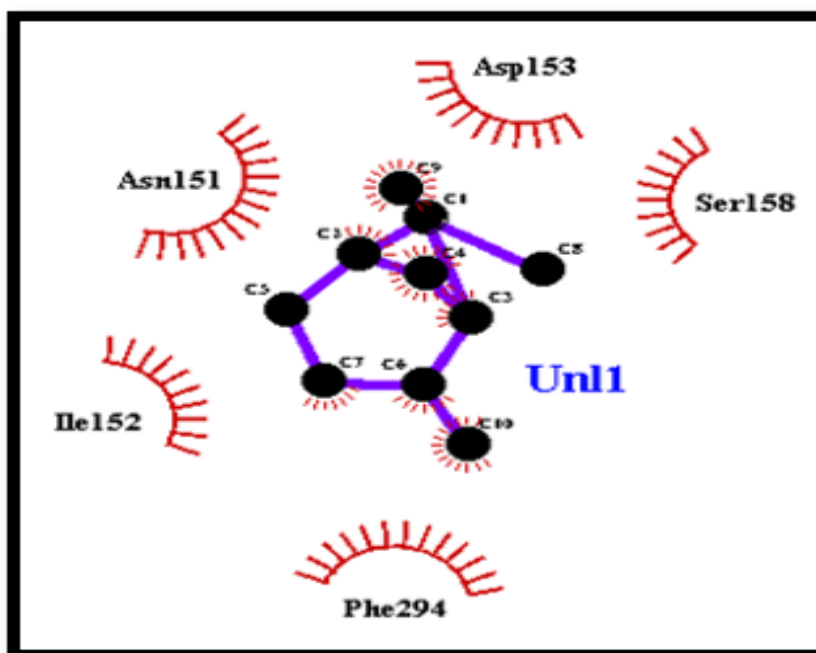


FIGURE 4.22: 2D structure showing interaction of Beta-pinene with 3CL pro.

Figure 4.23 showed the interaction of thymol with 3 CL protease. It showed that thymol had formed two hydrophobic interaction and two hydrogen bond.

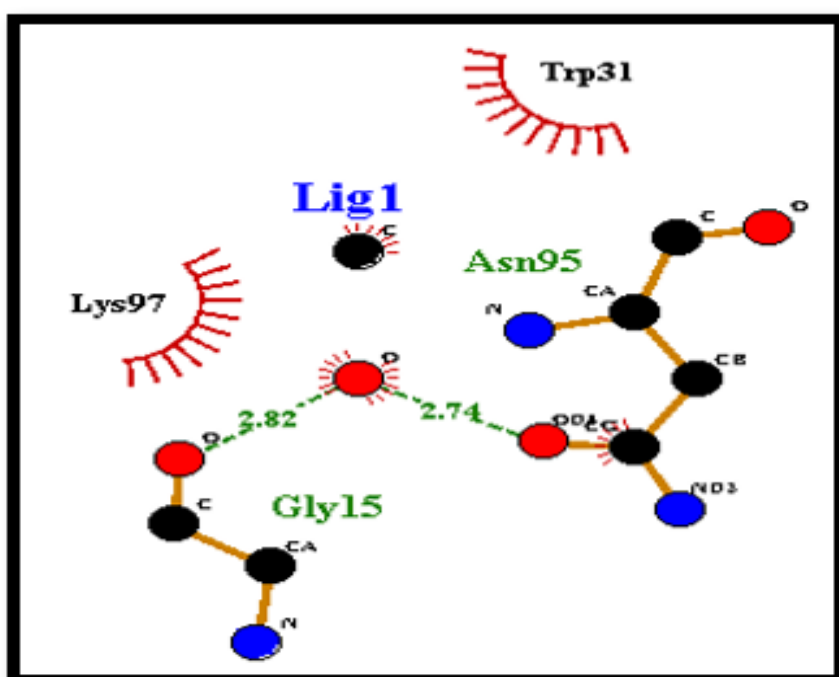


FIGURE 4.23: 2D structure showing interaction of Thymol with 3CL pro.

Figure 4.24 showed the interaction of thymol with 3 CL protease. It showed that thymol had formed two hydrophobic interaction and two hydrogen bond.

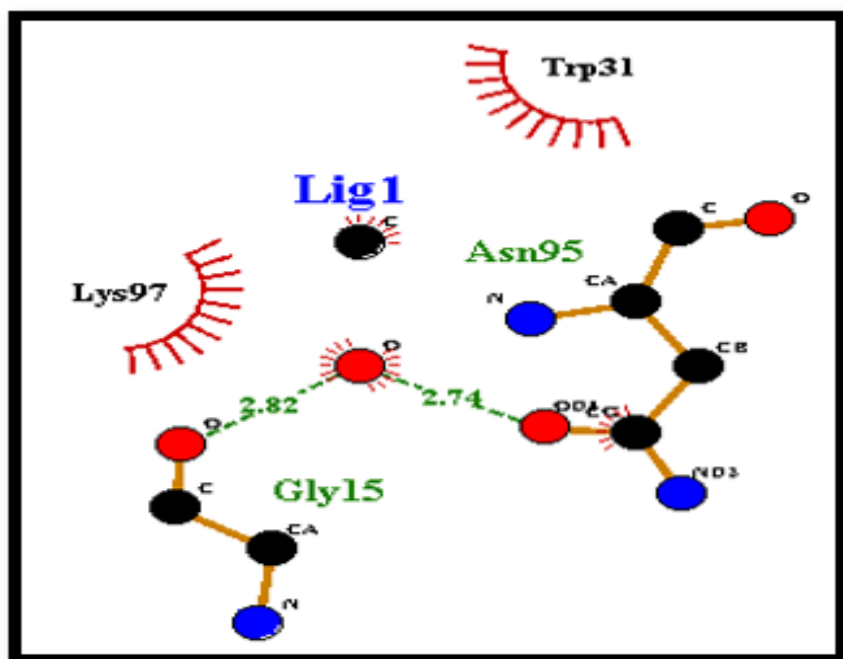


FIGURE 4.24: 2D structure showing interaction of Thymol with 3CL pro.

Figure 4.25 showed the interaction of carvacrol with 3 CL protease. It showed that carvacrol had formed no hydrophobic interaction and three hydrogen bond.

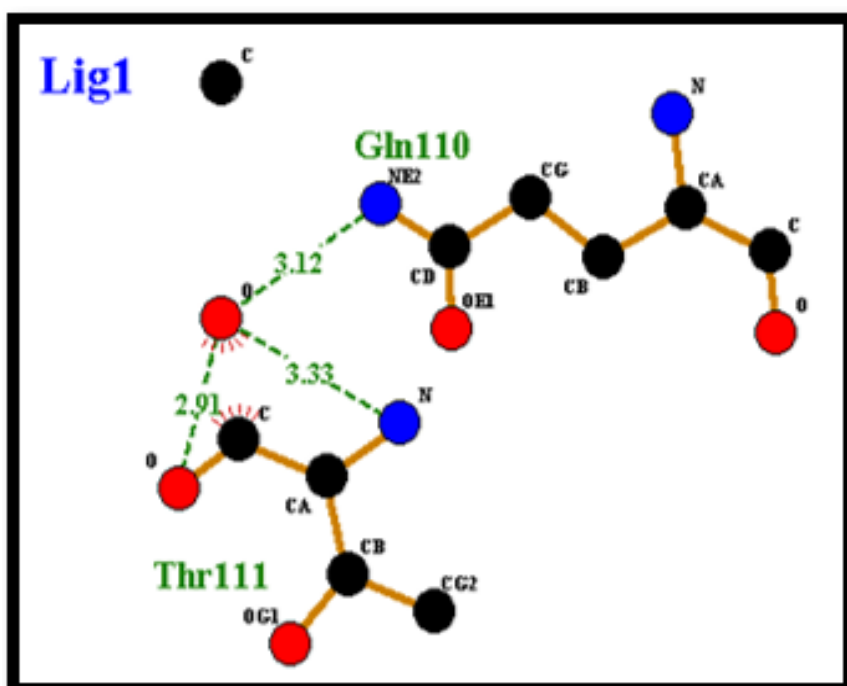


FIGURE 4.25: 2D structure showing interaction of Carvacrol with 3CL pro.

Figure 4.26 showed the interaction of p-cymene with 3 CL protease. It showed that p-cymene had formed one hydrophobic interaction but no hydrogen bond.

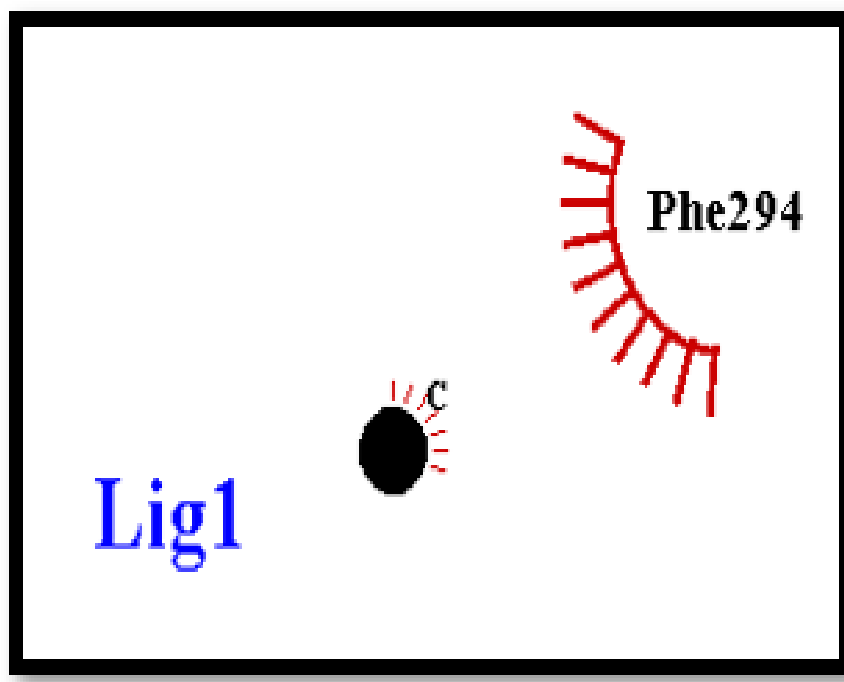


FIGURE 4.26: 2D structure showing interaction of P-cymene with 3CL pro.

Figure 4.27 showed the interaction of beta-pinene with 3 CL protease. It showed that beta-pinene had formed five hydrophobic interaction but no hydrogen bond.

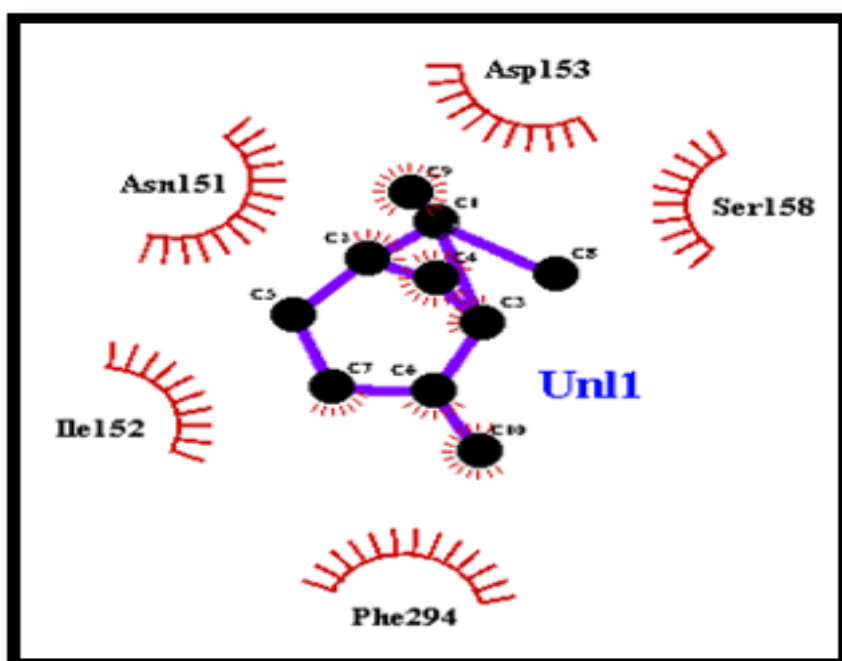


FIGURE 4.27: 2D structure showing interaction of Beta-pinene with 3CL pro.

Figure 4.28 showed the interaction of terpinene-4-ol with 3 CL protease. It showed that terpinene-4-ol had formed one hydrophobic interaction and one hydrogen bond.

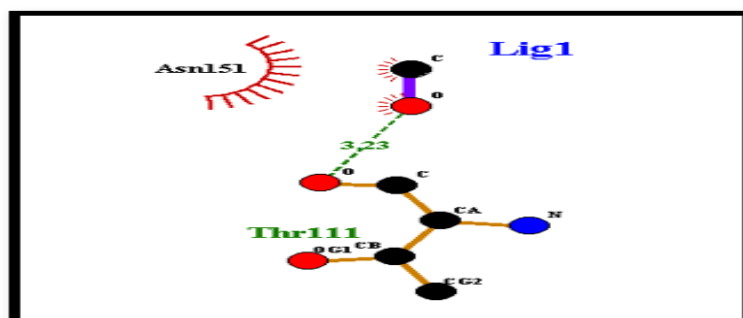


FIGURE 4.28: 2D structure showing interaction of Terpinene-4-ol with 3CL pro.

The details of the selected ligands' hydrogen and hydrophobic interactions with the receptor protein were shown in the table 4.9 below. It showed the binding scores, number of hydrogen bonds, amino acids and distance of the bond they formed and number of hydrophobic interactions they made.

TABLE 4.9: Selected ligands showing hydrogen bonding and hydrophobic interactions.

Ligands	Binding Score	H-bonds	Hydrogen Bonding	Hydrophobic Bonding	
			Amino Acids	Distance	
			NH2-		
			Gln110-		
			O	3.12	
			O-		
Carv-	-5.3	3	Thr111-	3.33	-
acrol			N		
			O-	2.91	
			Thr111-		
			O		

TABLE 4.9: Selected ligands showing hydrogen bonding and hydrophobic interactions.

Ligands	Binding Score	H-bonds	Hydrogen Bonding	Hydrophobic Bonding
			Amino Acids	Distance
Thymol	-5	2	O-Asn95- O	2.74 Trp31
			O-Gly15- O	2.82 Lys97
Alpha-terpineol	-5.3	2	O-Met17- O	3.03 Trp31
			O-Gly15- O	2.99 Ala70
				Gln110
				Asn151
Gamma-terpineol	-5.2	1	OG1-Thr111- O1	3.08 Ser158
				Asp153
				Phe294
				Thr122

TABLE 4.9: Selected ligands showing hydrogen bonding and hydrophobic interactions.

Ligands	Binding Score	H-bonds	Hydrogen Bonding		Hydrophobic Bonding
			Amino Acids	Distance	
Linalool	-4.9	1	O- His164-	3.20	His41
			O		Val104
					Ser158
Beta-caryophyllene	-5.9	0	-	-	Ile152
					Asp153
					Phe294
					Asn151
					Ile106
					Arg131
					Asp389
Piperine	-7	2	OZ- Lys137-		Gln390
			O1	3.10	Gln388
			CO- Leu287-	3.17	Tbr199
			N		Len386
					Tyr339
					Thr342

TABLE 4.9: Selected ligands showing hydrogen bonding and hydrophobic interactions.

Ligands	Binding Score	H-bonds	Hydrogen Bonding	Hydrophobic Bonding
			Amino Acids	Distance
Sabinene	-5	0	-	-
				Ser158
				Asp153
Beta-pinene	-4.7	0	-	-
				Asn151
				Ile152
				Phe294
Alpha-copaene	-6	0	-	-
			O1-Gln110-OD	Asp153
				2.97
Cinnamaldehyde	-5.2	3	O1-Thr111-O	Aso151
				Tbt393
				2.91
			O1-Thr111-OG1	Pbe294

TABLE 4.9: Selected ligands showing hydrogen bonding and hydrophobic interactions.

Ligands	Binding Score	H-bonds	Hydrogen Bonding	Amino Acids	Distance	Hydrophobic Bonding
Linalool	-4.9	1	O- His164- O	3.20	His41 Val104 Ser158 Ile152 Asp153 Phe294 Asn151 Phe8 Ile152	
Beta-caryophyllene	-5.9	0	-	-		
Eucalyptol	-5.1	-	-	-	Ser158 Asp153 Asn151	

TABLE 4.9: Selected ligands showing hydrogen bonding and hydrophobic interactions.

Ligands	Binding Score	H-bonds	Hydrogen Bonding	Hydrophobic Bonding
			Amino Acids	Distance
Eugenol	-5.5	1	NE2- Gln110- O	3.12 Asn151 Asp153
Cumin- aldehyde	-5.2	2	O1- Thr111- N	3.06 Ile152 Asn151
			O1- Thr111- OG1	2.81 Gln110 Thr292
P- Cymene	-5.1	-	-	- Phe294 Asp153
Beta- pinene	-4.7	0	-	- Asn151 Ile152 Phe294

TABLE 4.9: Selected ligands showing hydrogen bonding and hydrophobic interactions.

Ligands	Binding Score	H-bonds	Hydrogen Bonding	Hydrophobic Bonding	
			Amino Acids	Distance	
Gamma-terpinene	-5.1	-	-	-	Phe294
Thymol	-5	2	O-Asn95-	2.74	Trp31
			O-Gly15-	2.82	Lys97
Thymol	-5	2	O-Asn95-	2.74	Trp31
			O-Gly15-	2.82	Lys97
			NH2-Gln110-		Ser158
			O	3.12	Asp153
Carvacrol	-5.3	3	O-Thr111-	3.33	Asn151
			N		Ile152
			O-Thr111-	2.91	
			O		Phe294
					Thr234

TABLE 4.9: Selected ligands showing hydrogen bonding and hydrophobic interactions.

Ligands	Binding Score	H-bonds	Hydrogen Bonding	Amino Acids	Distance	Hydrophobic Bonding
P-cymene	-5.1	-	-	-	-	Phe294
						Ser158
						Asp153
Beta-pinene	-4.7	0	-	-	-	Asn151
						Ile152
						Phe294
Terpinene-4-ol	-4.7	1	O-Thr111-O	3.23		Asn151

4.9 ADMET Properties of Ligands

ADMET properties of ligands were identified via pkCSM online tool by putting input (ligands) as SMILES. ADMET properties describes the influence of drug level, kinetics and pharmacological activity of a compound that would be used as drug [81]. ADMET (Absorption, Distribution, Metabolism, Excretion, Toxicity) properties of selected compounds were shown in Table 4.10 to Table 4.16.

4.9.1 Absorption

The CaCO_2 solubility aids in the prediction of drug absorption when administered orally. High CaCO_2 permeability is defined as a value greater than 0.90 (log Papp in 10^{-6} cm/s).

The ligands' water solubility is given in log mol/L. This represents the compound's water solubility at 25° C. As a result, drugs that are lipid-soluble will be less soluble than drugs that are water-soluble.

Intestinal absorption is the amount of a compound that is absorbed in the intestines. A value of less than 30P-glycoprotein is an ABC transporter that functions as a biological barrier to expel toxins or other xenobiotics from cells.

P-glycoprotein inhibition can either be a therapeutic target or act in opposition. Skin permeability is essential for the creation of transdermal drugs. Skin permeability is low for any compound with a value greater than -2.5. Table 4.10 and table 4.11 showed all the absorptive properties of selected ligands [77].

TABLE 4.10: a) Absorptive properties of selected ligands.

Ligands	Water Solubility	CaCO_2 Permeability	Intestinal Absorption	Skin Permeability
Carvacrol	-2.789	1.606	90.84	-1.62
Thymol	-2.789	1.606	90.84	-1.62
Alpha-terpineol	-2.039	1.489	94.18	-2.418
Gamma-terpineol	-2.123	1.49	93.426	-2.41
Linalool	-2.612	1.49	93.16	-1.737
Beta-caryophyllene	-5.555	1.423	94.84	-1.58
Piperine	-3.464	1.596	94.44	-3.131
Sabinene	-4.629	1.404	95.35	-1.342

TABLE 4.10: a) Absorptive properties of selected ligands.

Ligands	Water Solubility	CaCO₂ Permeability	Intestinal Absorption	Skin Permeability
Beta- pinene	-4.191	1.385	95.52	-1.653
Alpha- copaene	-5.705	1.374	96.22	-2.225
Cinnam- aldehyde	-2.175	1.634	95.01	-2.355
Linalool	-2.612	1.49	93.16	-1.737
Beta- caryo- phyllene	-5.555	1.432	94.84	-1.58
Eucaly- ptol	-2.63	1.485	96.50	-2.437
Eugenol	-2.25	1.559	92.04	-2.207
Cumin- aldehyde	-2.96	1.609	95.84	-1.196
P- Cymene	-4.081	1.527	93.54	-1.192
Beta- pinene	-4.191	1.385	95.52	-1.653

TABLE 4.11: b) Absorptive properties of selected ligands.

Ligands	P Glycoprotein Substrate	P Glycoprotein I Inhibitor	P Glycoprotein II Inhibitor
Carvacrol	Nil	Nil	Nil
Thymol	Nil	Nil	Nil

TABLE 4.11: b) Absorptive properties of selected ligands.

Ligands	P Glycoprotein Substrate	P Glycoprotein I Inhibitor	P Glycoprotein II Inhibitor
Alpha-terpineol	Yes	Nil	Nil
Gamma-terpineol	Yes	Nil	Nil
Linalool	Nil	Nil	Nil
Beta-caryophyllene	Nil	Nil	Nil
Piperine	Yes	Yes	Nil
Sabinene	Nil	Nil	Nil
Beta-pinene	Nil	Nil	Nil
Alpha-copaene	Nil	Nil	Nil
Cinnamaldehyde	Nil	Nil	Nil
Linalool	Nil	Nil	Nil
Beta-caryophyllene	Nil	Nil	Nil
Eucalyptol	Yes	Nil	Nil
Eugenol	Nil	Nil	Nil
Cuminaldehyde	Nil	Nil	Nil

TABLE 4.11: b) Absorptive properties of selected ligands.

Ligands	P	P	P
	Glycoprotein Substrate	Glycoprotein I Inhibitor	Glycoprotein II Inhibitor
P-Cymene	Nil	Nil	Nil
Beta-pinene	Nil	Nil	Nil

Table 4.10 and 4.11 showed that almost all the ligands showed good absorptive properties. Intestinal absorption of all the ligands was appropriate. All the ligands were skin permeable. Results predicted that ligands doesnot inhibit the p-glycoprotein. Alpha-terpineol, gamma-terpineol, piperine and eucalyptol act as p-glycoprotein substrate.

4.9.2 Distribution

The VD_{ss} is the theoretical volume that describes the total dose of the drug that must be distributed uniformly to achieve the same concentration as in blood plasma. If the VD_{ss} value is greater than 2.81 L/kg, the drug is more concentrated in the tissues than in the plasma. If the value is less than 0.71 L/kg, the VD_{ss} is low. Many drugs in plasma exist in an equilibrium with the serum proteins, alternating between bound and unbound states. As a drug binds more to serum proteins, its diffusion efficiency to cellular membranes decreases. The blood-brain barrier protects the brain and reduces the ability of external compounds to enter the brain directly. If a compound has a logBB value greater than 0.3, it will easily cross the BBB barrier and thus be effective and if it is logBB < -1 then it is poorly distributed. Compounds with logPS > -2 penetrate the CNS, whereas logPS < -3 does not [77]. Table 4.12 below showed the distributive properties of selected ligands.

TABLE 4.12: Distributive properties of selected ligands.

Ligands	VD_{ss}	Fraction Unbound	BBB Permeability	CNS Permeability
Carv- acrol	0.512	0.203	0.407	-1.664
Thymol	0.512	0.203	0.407	-1.664
Alpha- terpineol	0.207	0.565	0.305	-2.807
Gamma- terpineol	0.189	0.558	0.3	-2.744
Linalool	0.152	0.484	0.598	-2.339
Beta- caryoph- yllene	0.652	0.263	0.733	-2.172
Piperine	0.158	0.134	-0.102	-1.879
Sabinene	0.566	0.295	0.836	-1.463
Beta- pinene	0.685	0.35	0.818	-1.857
Alpha- copaene	0.806	0.115	0.887	-1.659
Cinnam- aldehyde	0.266	0.3	0.436	-1.582
Linalool	0.152	0.484	0.598	-2.339
Beta- caryo- phyllene	0.652	0.263	0.733	-2.172
Eucal- yptol	0.491	0.553	0.368	-2.972
Eugenol	0.24	0.251	0.374	-2.007
Cumin- aldehyde	0.324	0.263	0.438	-1.485

TABLE 4.12: Distributive properties of selected ligands.

Ligands	VDss	Fraction Unbound	BBB Permeability	CNS Permeability
P- Cymene	0.697	0.159	0.478	-1.39
Beta- pinene	0.685	0.35	0.818	-1.857
Gamma- terpinene	0.412	0.42	0.754	-2.049
Thymol	0.512	0.203	0.407	-1.664
Thymol	0.512	0.203	0.407	-1.664
Carvacrol	0.512	0.203	0.407	-1.664
P- cymene	0.697	0.159	0.478	-1.397
Beta- pinene	0.685	0.35	0.818	-1.857
Terpin- ene-4-ol	0.21	0.514	0.563	-2.473

Table 4.12 showed that all the ligands had VDss amount in appropriate manner. BBB permeability of some of the ligands was more than -1 and less than 0.3 while other deviated. All the ligands have CNS permeability less than -3.

4.9.3 Metabolism

Cytochrome P450 is a liver detoxification enzyme. This enzyme deactivates many drugs, but it can also activate others. Inhibitors of this enzyme can directly affect drug metabolism and should not be used. Likewise, CYP2D6 and CYP3A4 are in charge of drug metabolism. Inhibition of these has an effect on the pharmacokinetics of the drug under consideration [77]. The table 4.13 below showed the metabolic properties of the selected ligands.

TABLE 4.13: Metabolic properties of selected ligands.

Ligands	CYP2D6- Substrate	CYP3A4- Substrate	CYP1A2- Inhibitor	CYP2C19- Inhibitor	CYP2C9- Inhibitor	CYP2D6- Inhibitor	CYP3A4- Inhibitor
Carv- acrol	Nil	Nil	Yes	Nil	Nil	Nil	Nil
Thymol	Nil	Nil	Yes	Nil	Nil	Nil	Nil
Alpha- terpineol	Nil	Nil	Nil	Nil	Nil	Nil	Nil
Gamma- terpineol	Nil	Nil	Nil	Nil	Nil	Nil	Nil
Linalool	Nil	Nil	Nil	Nil	Nil	Nil	Nil
Beta- caryo- phyllene	Nil	Nil	Nil	Nil	Nil	Nil	Nil
Piperine	Nil	Yes	Nil	Yes	Nil	Nil	Nil
Sabinene	Nil	Nil	Nil	Nil	Nil	Nil	Nil
Beta- pinene	Nil	Nil	Nil	Nil	Nil	Nil	Nil

TABLE 4.13: Metabolic properties of selected ligands.

Ligands	CYP2D6- Substrate	CYP3A4- Substrate	CYP1A2- Inhibitor	CYP2C19- Inhibitor	CYP2C9- Inhibitor	CYP2D6- Inhibitor	CYP3A4- Inhibitor
Alpha-copaene	Nil	Yes	Yes	Nil	Nil	Nil	Nil
Cinnamaldehyde	Nil	Nil	Yes	Nil	Nil	Nil	Nil
Linalool	Nil	Nil	Nil	Nil	Nil	Nil	Nil
Beta-caryophyllene	Nil	Nil	Nil	Nil	Nil	Nil	Nil
Eucalyptol	Nil	Nil	Nil	Nil	Nil	Nil	Nil
Eugenol	Nil	Nil	Yes	Nil	Nil	Nil	Nil
Cuminaldehyde	Nil	Nil	Yes	Nil	Nil	Nil	Nil
P-Cymene	Nil	Nil	Yes	Nil	Nil	Nil	Nil

TABLE 4.13: Metabolic properties of selected ligands.

Ligands	CYP2D6- Substrate	CYP3A4- Substrate	CYP1A2- Inhibitor	CYP2C19- Inhibitor	CYP2C9- Inhibitor	CYP2D6- Inhibitor	CYP3A4- Inhibitor
Beta- pinene	Nil	Nil	Nil	Nil	Nil	Nil	Nil
Gamma- terpinene	Nil	Nil	Nil	Nil	Nil	Nil	Nil
Thymol	Nil	Nil	Yes	Nil	Nil	Nil	Nil
Thymol	Nil	Nil	Yes	Nil	Nil	Nil	Nil
Carv- acrol	Nil	Nil	Yes	Nil	Nil	Nil	Nil
P- cymene	Nil	Nil	Yes	Nil	Nil	Nil	Nil
Beta- pinene	Nil	Nil	Nil	Nil	Nil	Nil	Nil
Terpin- ene-4-ol	Nil	Nil	Nil	Nil	Nil	Nil	Nil

Table 4.13 showed that CYP2D6-substrate was not present in any ligand while CYP3A4 –substrate was present only in piperine and alpha-coapane. CYP1A2-inhibitors were carvacrol, thymol, alpha-coapane, eugenol, cinnamaldehyde, cuminaldehyde and p-cymene. CYP2C19- inhibitors was only piperine. CYP2C9-inhibitor, CYP2D6- inhibitor, CYP3A4- inhibitor were not present in any ligand.

4.9.4 Excretion

The Renal OCT2 substrate functions as a transporter, assisting in the elimination of drugs and other compounds. Total clearance denotes hepatic clearance, which means the drug is metabolized, whereas renal clearance denotes excretion [77].

Excretory properties were shown in Table 4.14 below.

TABLE 4.14: Excretory properties of selected ligands.

Ligands	Total Clearance	Renal OCT2-Substrate
Carvacrol	0.207	Nil
Thymol	0.211	Nil
Alpha-terpineol	1.219	Nil
Gamma-terpineol	1.222	Nil
Linalool	0.446	Nil
Beta-caryophyllene	1.088	Nil
Piperine	0.232	Yes
Sabinene	0.071	Nil
Beta-pinene	0.03	Nil
Alpha-copaene	0.95	Nil
Cinnamaldehyde	0.203	Nil
Linalool	0.446	Nil
Beta-caryophyllene	1.088	Nil
Eucalyptol	1.009	Nil
Eugenol	0.282	Nil
Cuminaldehyde	0.227	Nil

TABLE 4.14: Excretory properties of selected ligands.

Ligands	Total Clearance	Renal OCT2-Substrate
P-Cymene	0.239	Nil
Beta-pinene	0.03	Nil
Gamma-terpinene	0.217	Nil
Thymol	0.211	Nil
Thymol	0.211	Nil
Carvacrol	0.207	Nil
P-cymene	0.239	Nil
Beta-pinene	0.03	Nil
Terpinene-4-ol	1.269	Nil

The table 4.14 showed that all the ligands except piperine does not have OCT2 Renal substrate which indicates that they would not be cleared out of the body. Total clearance values of all the ligands were also given accordingly.

4.9.5 Toxicity

The AMES toxicity test employs bacteria to assess the compound's mutagenic potential. If it responds positively, the ligand is mutagenic and may also act as a carcinogen.

T. Pyriformis (protozoa bacteria) toxicity is used as a toxic endpoint in the *T. Pyriformis* toxicity method. Any value greater than $-0.5 \log \mu\text{g/L}$ is known to be toxic. The Minnow toxicity test predictions are used to depict the concentration at which the compound could kill 50% of the minnows. A value less than 0.5 mM is considered acutely toxic.

The MRTD (maximum recommended tolerated dose) values depict the starting dose of a specific pharmaceutical during clinical phase I. A value of 0.477 $\log \text{mg/kg/day}$ is considered low, while a value greater than this is considered high.

For the oral rat chronic toxicity test, the predicted log value of the lowest observed adverse effect in log-mg/kg bw/day is given, which relates to the compound concentration required for the treatment time.

A hepatotoxicity test predicts whether or not a compound will have an effect on the liver's function.

A skin test estimates whether or not the compound will cause skin reactions. The hERG I and II inhibitor test determines whether a compound has the potential to inhibit the potassium channels linked with hERG. An inhibitor of these channels may cause QT syndrome, and in the long term, the person may develop ventricular arrhythmia [77]. The toxicity prediction was shown in Table 4.15 and 4.16 below.

TABLE 4.15: a) Toxicity prediction of selected ligands.

Ligands	<i>T.Pyriformis</i> Toxicity	Minnows Toxicity
Carvacrol	0.387	1.213
Thymol	0.387	1.213
Alpha-terpineol	0.008	1.8
Gamma-terpineol	-0.019	1.87
Linalool	0.515	1.277
Beta-caryophyllene	1.401	0.504
Piperine	1.879	1.732

TABLE 4.15: a) Toxicity prediction of selected ligands.

Ligands	<i>T.Pyriformis</i> Toxicity	Minnows Toxicity
Sabinene	0.788	0.726
Beta- pinene	0.628	1.012
Alpha- copaene	1.122	0.128
Cinnam- aldehyde	0.665	1.605
Linalool	0.515	1.277
Beta- caryo- phyllene	1.401	0.504
Eucaly- ptol	0.171	1.735
Euge- nol	0.3	1.702

The table 4.15 and 4.16 showed the toxicity values of the selected ligands. AMES toxicity had only shown by eugenol which means it will be carcinogenic. hERG inhibitors are not present in any ligand. Some ligands had shown hepato-toxicity which means they may be harmful to liver. Some ligands are sensitive to skin while other are not. *T.Pyriformis* toxicity was not present in any ligand. Minnows toxicity was shown only in alpha-coapane.

TABLE 4.16: b) Toxicity prediction of selected ligands.

Ligands	AMES Toxicity	Max. Tolerated Dose	hERG I Inhibitor	hERG II Inhibitor	Oral	Oral	Hepato Toxicity	Skin Sensitisation
					Rat Acute Toxicity	Rat Chronic Toxicity		
Carvacrol	Nil	1.007	Nil	Nil	2.074	2.212	Yes	Yes
Thymol	Nil	1.007	Nil	Nil	2.074	2.212	Yes	Yes
Alpha- terpineol	Nil	0.886	Nil	Nil	1.923	1.945	Nil	Yes
Gamma- terpineol	Nil	0.861	Nil	Nil	1.909	2.032	Nil	Yes
Linalool	Nil	0.774	Nil	Nil	1.704	2.024	Nil	Yes
Beta- caryo- phyllene	Nil	0.351	Nil	Nil	1.617	1.416	Nil	Yes
Piperine	Nil	-0.38	Nil	Nil	2.811	1.51	Yes	Nil
Sabinene	Nil	0.369	Nil	Nil	1.549	2.309	Nil	Nil
Beta- pinene	Nil	0.371	Nil	Nil	1.673	2.28	Nil	Nil

TABLE 4.16: b) Toxicity prediction of selected ligands.

Ligands	AMES Toxicity	Max. Tolerated Dose	hERG I Inhibitor	hERG II Inhibitor	Oral Rat Acute Toxicity	Oral Rat Chronic Toxicity	Hepato Toxicity	Skin Sensitisation
Alpha- copaene	Nil	-0.302	Nil	Nil	1.644	1.356	Nil	Nil
Cinnam- aldehyde	Nil	0.876	Nil	Nil	1.88	1.944	Nil	Yes
Linalool	Nil	0.774	Nil	Nil	1.704	2.024	Nil	Yes
Beta- caryo- phyllene	Nil	0.351	Nil	Nil	1.617	1.416	Nil	Yes
Eucaly- ptol	Nil	0.553	Nil	Nil	2.01	2.029	Nil	Yes
Euge- nol	Yes	1.024	Nil	Nil	2.118	2.049	Nil	Yes

4.10 Lead Compound Identification

The physiochemical and pharmacokinetic properties of ligands determine whether or not they are drug or non-drug compounds. The first filter for this identification is Lipinski's rule, and the second filter is pharmacokinetics. After detailed analysis of protein ligand interaction, binding score and pharmacokinetic properties of selected ligands, ligands with best results were selected from different spices Gamma-terpineol from oregano, piperine from black pepper, cinnamaldehyde from cinnamon, cuminaldehyde from cumin and terpinen-4-ol from ajwain.

4.11 Selection of Antiviral Drug

The most effective antiviral drug had been chosen based on its physiochemical, ADMET, and mechanism of action with side effects. For physiochemical properties, the online database PubChem was used, and for ADMET properties, the online tool pkCSM was used. When the disease first appeared, many FDA-approved drugs were used for drug repurposing in order to find the best treatment against the virus. Remdesivir is a prodrug of an ATP analogue that may have antiviral activity against COVID-19 caused by SARS-CoV-2. Remdesivir has an FDA Emergency Use Authorization for use in adults and children in the hospital with suspected or confirmed COVID-19 and a SpO₂ of 94 Mechanism of action was identified by KEGG. Physiochemical properties of antiviral drug Remdesivir were shown in Table 4.17.

TABLE 4.17: Physiochemical properties of Remdesivir.

Chemical Formula	Molecular Weight	Log P Value
C ₂₇ H ₃₅ N ₆ O ₈ P	602.58	2.31218
HBD	HBA	Rotatable Bonds
4	13	13

The table 4.17 showed the molecular weight, log P value, hydrogen bond acceptor, hydrogen bond donor, and rotatable bonds present in Remdesivir.

4.12 Mechanism of Action of Remdesivir

The chosen medicine Remdesivir's mechanism of action was determined utilising the internet database KEGG. Remdesivir enters cells and is cleaved to its monophosphate form by carboxylesterase 1 or cathepsin A before being phosphorylated by unidentified kinases to produce its active triphosphate form, remdesivir triphosphate (RDV-TP). RDV-TP is efficiently integrated into the SARS-CoV-2 RdRp complex. Remdesivir has a free 3'-hydroxyl group, which allows for chain lengthening.

However, modelling and in vitro experiments show that the 1-cyano group collision of remdesivir with RdR's Ser-861 at I + 4 (corresponding to the position of the fourth nucleotide incorporation after RDV-TP) prevents translocation and terminates replication at I + 3 position [82]. Remdesivir as an adenosine analogue that can target the RNA-dependent RNA polymerase (RdRp) and inhibit viral RNA synthesis. 3CLpro is an important CoV protease that cleaves the large replicase polyproteins during viral replication and can be targeted by the protease inhibitors.

4.13 Remdesivir Effects on Body

There is limited information regarding safety and effectiveness of using Remdesivir to treat patients of COVID-19. Remdesivir was firstly developed by manufacturers for hepatitis C, and later tried on the virus that causes Ebola. Some study results showed that remdesivir may help some patients get better soon [82].

Beside these positive effects Remdesivir may cause some negative effects in body as nausea, vomiting, sweating and low blood pressure. In case of serious allergic reactions rash, itching, dizziness, temperature fluctuation & difficulty in breathing.

4.14 ADMET Properties of Selected Drug

ADMET properties of ligands were identified via pkCSM online tool by putting input (ligands) as SMILES. ADMET properties describes the influence of drug level, kinetics and pharmacological activity of a compound that would be used as drug [81]. ADMET properties of selected compounds are shown in Table 4.18 below.

In absorptive properties, the CaCO₂ solubility aids in the prediction of drug absorption when administered orally. High CaCO₂ permeability is defined as a value greater than 0.90 (log Papp in 10⁻⁶ cm/s). The ligands' water solubility is given in log mol/L. This represents the compound's water solubility at 25°C. As a result, drugs that are lipid-soluble will be less soluble than drugs that are water-soluble. Intestinal absorption is the amount of a compound that is absorbed in the intestines. A value of less than 30% is considered inadequately absorbed. P-glycoprotein is an ABC transporter that functions as a biological barrier to expel toxins or other xenobiotics from cells. P-glycoprotein inhibition can either be a therapeutic target or act in opposition. Skin permeability is essential for the creation of transdermal drugs. Skin permeability is low for any compound with a value greater than -2.5 [77].

In distributive properties, the VD_{ss} is the theoretical volume that describes the total dose of the drug that must be distributed uniformly to achieve the same concentration as in blood plasma. If the VD_{ss} value is greater than 2.81 L/kg, the drug is more concentrated in the tissues than in the plasma. If the value is less than 0.71 L/kg, the VD_{ss} is low. Many drugs in plasma exist in an equilibrium with the serum proteins, alternating between bound and unbound states. As a drug binds more to serum proteins, its diffusion efficiency to cellular membranes decreases. The blood-brain barrier protects the brain and reduces the ability of external compounds to enter the brain directly. If a compound has a logBB value greater than 0.3, it will easily cross the BBB barrier and thus be effective and if it is logBB < -1 then it is poorly distributed. Compounds with logPS > -2 penetrate the CNS, whereas logPS < -3 does not [77]. In metabolic properties, Cytochrome P450

is a liver detoxification enzyme. This enzyme deactivates many drugs, but it can also activate others. Inhibitors of this enzyme can directly affect drug metabolism and should not be used. Likewise, CYP2D6 and CYP3A4 are in charge of drug metabolism. Inhibition of these has an effect on the pharmacokinetics of the drug under consideration [77].

In excretory properties, the Renal OCT2 substrate functions as a transporter, assisting in the elimination of drugs and other compounds. Total clearance denotes hepatic clearance, which means the drug is metabolized, whereas renal clearance denotes excretion [77].

In toxicity prediction, the AMES toxicity test employs bacteria to assess the compound's mutagenic potential. If it responds positively, the ligand is mutagenic and may also act as a carcinogen. *T. Pyriformis* (protozoa bacteria) toxicity is used as a toxic endpoint in the *T. Pyriformis* toxicity method. Any value greater than $-0.5 \log \mu\text{g/L}$ is known to be toxic.

The Minnow toxicity test predictions are used to depict the concentration at which the compound could kill 50% of the minnows. A value less than 0.5 mM is considered acutely toxic.

The MRTD (Maximum Recommended Tolerated Dose) values depict the starting dose of a specific pharmaceutical during clinical phase I. A value of 0.477 log mg/kg/day is considered low, while a value greater than this is considered high. For the oral rat chronic toxicity test, the predicted log value of the lowest observed adverse effect in log-mg/kg bw/day is given, which relates to the compound concentration required for the treatment time. A hepatotoxicity test predicts whether or not a compound will have an effect on the liver's function. A skin test estimates whether or not the compound will cause skin reactions.

The hERG I and II inhibitor test determines whether a compound has the potential to inhibit the potassium channels linked with hERG. An inhibitor of these channels may cause QT syndrome, and in the long term, the person may develop ventricular arrhythmia [77]. ADMET properties of Remdesevir were shown in Table 4.18.

TABLE 4.18: Showed the ADMET properties of remdesivir

ADMET Properties	Properties	Remdesivir
Absorption	Water Solubility	-3.07
	Caco2 Permeability	0.635
	Intestinal Absorption	71.10
	Skin Permeability	-2.735
	P Glycoprotein Substrate	Yes
	P Glycoprotein Inhibitor	Yes
	P Glycoprotein Inhibitor	Nil
	VDss	0.307
	Fraction Unbound	0.005
	BBB Permeability	-2.056
Distribution	CNS Permeability	-4.675

TABLE 4.18: Showed the ADMET properties of remdesivir

ADMET Properties	Properties	Remdesivir	
Metabolism	CYP2D6-Substrate	Nil	
	CYP3A4-Substrate	Yes	
	CYP1A2-Inhibitor	Nil	
	CYP2C19-Inhibitor	Nil	
	CYP2C9-Inhibitor	Nil	
	CYP2D6-Inhibitor	Nil	
	CYP3A4-Inhibitor	Nil	
	Total Clearance	0.198	
	Excretion	OCT2-Substrate	Nil
		AMES-Toxicity	Nil
Max. tolerated-Dose		0.15	
Toxicity		hERG I-Inhibitor	Nil

TABLE 4.18: Showed the ADMET properties of remdesivir

ADMET Properties	Properties	Remdesivir
	hERG	
	II-Inhibitor	Yes
	Oral	
	Rat	
	Acute-Toxicity (LD50)	2.043
	Oral	
	Rat	
	Chronic-Toxicity (LOAEL)	1.639
	Hepato-Toxicity	Yes
	Skin Sensitisation	Nil
	T. Pyriformis-Toxicity	0.285

4.15 Remdesivir Docking

CB Dock is online tool that was used for docking of Remdesivir (as ligand) and 3CLpro (as receptor). The result of docking was comprising of 5 best conformational poses and finest was selected. Docking results of selected protein-ligand

complex were shown in Table 4.19.

TABLE 4.19: Docking result of Remdesevir with 3CL protease.

Binding Score	Cavity Size
-8	258

The table 4.19 showed the binding score and cavity size of docked molecule of remdesevir and 3CL protease.

4.16 Comparison of Remedesevir and Best Ligand

This comparison helped us to identify the better treatment for COVID-19. It was based on following parameters like; ADMET that were absorption, distribution, metabolism, excretion and toxicity properties and physiochemical properties of Remdesivir and selected ligand.

Comparison of remdesevir with the lead compounds selected from five different spices.

4.16.1 Comparison of Physiochemical Properties and ADMET Properties

The comparison between the physiochemical and ADMET that were absorption, distribution, metabolism, excretion and toxicity properties of remdesevir and selected ligands was shown in table below.

It helped us in identifying whether the compounds we were predicting as a drug in alternate of standard drug were better in all properties or not. Either they are safe for use or not.

Comparison was shown in Table 4.20.

TABLE 4.20: Comparison of physiochemical and ADMET properties of lead compounds and remdesivir.

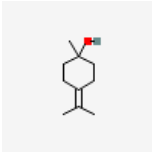
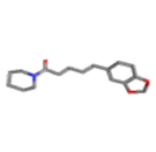
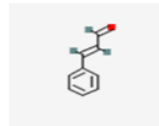
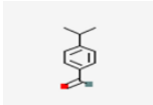
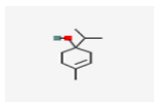
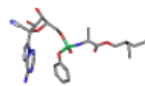
Properties		Gamma-terpineol	Piperine	Cinnamaldehyde	Cuminaldehyde	Terpinene-4-ol	Remdesivir
Physiochemical Properties	Molecular formula	C ₁₀ H ₁₈ O	C ₁₇ H ₁₉ N ₃ O	C ₉ H ₈ O	C ₁₀ H ₁₂ O	C ₁₀ H ₁₈ O	C ₂₇ H ₃₅ N ₆ O ₈ P
	Molecular weight	154.25	285.34	132.16	148.20	154.25	602.58
	Structure						
Lipinski Rule Of Five	Log P Value	2.6478	2.9972	1.8987	2.6225	2.5037	2.31218
	Molecular weight	154.25	285.34	132.16	148.20	154.25	602.58
	H Bond Acceptor	1	3	1	1	1	13
	H Bond Donor	1	0	0	0	1	4

TABLE 4.20: Comparison of physiochemical and ADMET properties of lead compounds and remdesivir.

	Properties	Gamma-terpineol	Piperine	Cinnamaldehyde	Cuminaldehyde	Terpinene-4-ol	Remdesivir
Absorption	Rotatable-Bonds	0	3	2	2	1	13
	Water Solubility	-2.123	-3.464	-2.175	-2.966	-2.296	-3.07
	Caco2 Permeability	1.49	1.596	1.634	1.609	1.502	0.635
	Intestinal Absorption	93.426	94.44	95.01	95.84	94.01	71.10
	Skin Permeability	-2.41	-3.131	-2.355	-1.196	-2.182	-2.735
	P glycoprotein substrate	Yes	Yes	Nil	Nil	Nil	Yes
	P glycoprotein I inhibitor	Nil	Yes	Nil	Nil	Nil	Yes

TABLE 4.20: Comparison of physiochemical and ADMET properties of lead compounds and remdesivir.

	Properties	Gamma-terpineol	Piperine	Cinnamaldehyde	Cuminaldehyde	Terpinene-4-ol	Remdesivir
Distribution	P glycoprotein	Nil	Nil	Nil	Nil	Nil	Nil
	II inhibitor						
	VDss	0.189	0.158	0.266	0.324	0.21	0.307
	Fraction Unbound	0.558	0.134	0.3	0.263	0.514	0.005
	BBB permeability	0.3	-0.102	0.436	0.438	0.563	-2.056
	CNS permeability	-2.744	-1.879	-1.582	-1.485	-2.473	-4.675
	CYP2D6-substrate	Nil	Nil	Nil	Nil	Nil	Nil
Metabolism	CYP3A4-substrate	Nil	Yes	Nil	Nil	Nil	Yes
	CYP1A2-inhibitor	Nil	Nil	Yes	Yes	Nil	Nil

TABLE 4.20: Comparison of physiochemical and ADMET properties of lead compounds and remdesivir.

	Properties	Gamma-terpineol	Piperine	Cinnamaldehyde	Cuminaldehyde	Terpinene-4-ol	Remdesivir
Excretion	CYP2C19-inhibitor	Nil	Yes	Nil	Nil	Nil	Nil
	CYP2C9-inhibitor	Nil	Nil	Nil	Nil	Nil	Nil
	CYP2D6-inhibitor	Nil	Nil	Nil	Nil	Nil	Nil
	CYP3A4-inhibitor	Nil	Nil	Nil	Nil	Nil	Nil
	Total clearance	1.222	0.232	0.203	0.227	1.269	0.198
	Renal						
	OCT2-substrate	Nil	Yes	Nil	Nil	No	Nil

TABLE 4.20: Comparison of physiochemical and ADMET properties of lead compounds and remdesivir.

	Properties	Gamma-terpineol	Piperine	Cinnamaldehyde	Cuminaldehyde	Terpinene-4-ol	Remdesivir
	AMES-	Nil	Nil	Nil	Nil	Nil	Nil
	Toxicity						
	Max.						
Toxicity	tolerated-dose	0.861	-0.38	0.876	0.839	0.857	0.15
	hERG I-inhibitor	Nil	Nil	Nil	Nil	Nil	Nil
	hERG II-inhibitor	Nil	Nil	Nil	Nil	Nil	Yes
	Oral						
	Rat						
	Acute-Toxicity (LD50)	1.909	2.811	1.88	1.7	1.811	2.043

TABLE 4.20: Comparison of physiochemical and ADMET properties of lead compounds and remdesivir.

Properties	Gamma-terpineol	Piperine	Cinnamaldehyde	Cuminaldehyde	Terpinene-4-ol	Remdesivir
Oral Rat Chronic-Toxicity (LOAEL)	2.032	1.51	1.944	2.194	2.02	1.639
Hepato-toxicity	Nil	Yes	Nil	Nil	Nil	Yes
Skin Sensitisation	Yes	Nil	Yes	Yes	Yes	Nil
<i>T. Pyriiformis</i> - <i>toxicity</i>	-0.019	1.879	0.665	0.766	0.189	0.285
Minnow- toxicity	1.87	1.732	1.605	0.819	1.545	0.291

4.16.2 Comparison of Docking Results

Comparison of docking results of remdesivir and selected ligands showed that whether the compounds we were predicting for drug base alternative against remdesivir are making good interactions with protein and binding score was good or not. Table 4.21 and 4.22 showed the docking results of selected ligands and remdesivir including binding score and cavity size.

TABLE 4.21: a) Comparison of docking result of remdesivir and lead compounds.

Properties		Gamma-terpineol	Piperine	Cinnamaldehyde
Docking Results	Binding score (kJ/m-1)	-5.2	-7	-5.2
	Cavity size	212	688	212

TABLE 4.22: b) Comparison of docking result of remdesivir and lead compounds.

	Cumin-aldehyde	Terpinene-4-ol	Remdesivir
Docking Results	-5.2	-4.7	-8
	212	212	258

Chapter 5

Conclusions and Recommendations

The purpose of this study was to identify several bioactive compounds derived from essential oils of various spices that could be used to inhibit the activity of 3CLpro of SARS-CoV-2. The majority of these compounds had good binding scores, ADMET properties, and low toxicity values. These compounds docked well with 3CLpro and abide to the Lipinski rule of five. After detailed analysis of physiochemical properties, ADMET prediction, docking results and Lipinski rule of five, gamma-terpineol from *Origanum vulgare*, piperine from *Piper nigrum*, cinnamaldehyde from *Cinnamomum verum*, cuminaldehyde from *Cuminum cyminum* and Terpinene-4-ol from *Trachyspermum ammi* were considered as lead compounds. Comparison of these ligands with Remdesivir shows that they were all recommended as potential inhibitors of 3CLprotease of COVID 19.

As there had some side effects seen after vaccination for COVID-19, so these active compounds from spices showed less toxicity and had good physiochemical and pharmacological properties. The findings indicate that these ligands were a promising sign for the development of COVID-19 antiviral medication. The findings of this study could be used to develop an antiviral drug against COVID-19 in the future with low toxicity and better binding score.

Bibliography

- [1] F. Wu, S. Zhao, B. Yu, Y.-M. Chen, W. Wang, Z.-G. Song, et al., "A new coronavirus associated with human respiratory disease in China," *Nature*, vol. 579, pp. 265-269, 2020.
- [2] G. Pellino and A. Spinelli, "How coronavirus disease 2019 outbreak is impacting colorectal cancer patients in Italy: a long shadow beyond infection," *Diseases of the Colon and Rectum*, vol. 63, pp. 720-722, 2020.
- [3] J. Machhi, J. Herskovitz, A. M. Senan, D. Dutta, B. Nath, M. D. Oleynikov, et al., "The natural history, pathobiology, and clinical manifestations of SARS-CoV-2 infections," *Journal of Neuroimmune Pharmacology*, pp. 1-28, 2020.
- [4] S. Hoehl, H. Rabenau, A. Berger, M. Kortenbusch, J. Cinatl, D. Bojkova, et al., "Evidence of SARS-CoV-2 infection in returning travelers from Wuhan, China," *New England Journal of Medicine*, vol. 382, pp. 1278-1280, 2020.
- [5] S. Bilgin, O. Kurtkulagi, G. B. Kahveci, T. T. Duman, B. Meryem, and A. Tel, "Millennium pandemic: A review of coronavirus disease (COVID-19)," *Experimental Biomedical Research*, vol. 3, pp. 117-126, 2020.
- [6] P. Zhou, X.-L. Yang, X.-G. Wang, B. Hu, L. Zhang, W. Zhang, et al., "A pneumonia outbreak associated with a new coronavirus of probable bat origin," *nature*, vol. 579, pp. 270-273, 2020.
- [7] D. D. Richman, R. J. Whitley, and F. G. Hayden, *Clinical virology: John Wiley and Sons*, 2020.

- [8] T. G. Ksiazek, D. Erdman, C. S. Goldsmith, S. R. Zaki, T. Peret, S. Emery, et al., "A novel coronavirus associated with severe acute respiratory syndrome," *New England journal of medicine*, vol. 348, pp. 1953-1966, 2003.
- [9] C. Drosten, S. Günther, W. Preiser, S. Van Der Werf, H.-R. Brodt, S. Becker, et al., "Identification of a novel coronavirus in patients with severe acute respiratory syndrome," *New England journal of medicine*, vol. 348, pp. 1967-1976, 2003.
- [10] R. J. De Groot, S. C. Baker, R. S. Baric, C. S. Brown, C. Drosten, L. Enjuanes, et al., "Commentary: Middle east respiratory syndrome coronavirus (mers-cov): announcement of the coronavirus study group," *Journal of virology*, vol. 87, pp. 7790-7792, 2013.
- [11] A. M. Zaki, S. Van Boheemen, T. M. Bestebroer, A. D. Osterhaus, and R. A. Fouchier, "Isolation of a novel coronavirus from a man with pneumonia in Saudi Arabia," *New England Journal of Medicine*, vol. 367, pp. 1814-1820, 2012.
- [12] B. Benarba and A. Pandiella, "Medicinal plants as sources of active molecules against COVID-19," *Frontiers in pharmacology*, vol. 11, p. 1189, 2020.
- [13] L. Pelkmans and A. Helenius, "Insider information: what viruses tell us about endocytosis," *Current opinion in cell biology*, vol. 15, pp. 414-422, 2003.
- [14] S. B. Siczarski and G. R. Whittaker, "Dissecting virus entry via endocytosis," *Journal of General Virology*, vol. 83, pp. 1535-1545, 2002.
- [15] Z. Qinfen, C. Jinming, H. Xiaojun, Z. Huanying, H. Jicheng, F. Ling, et al., "The life cycle of SARS coronavirus in Vero E6 cells," *Journal of medical virology*, vol. 73, pp. 332-337, 2004.
- [16] Z.-Y. Yang, Y. Huang, L. Ganesh, K. Leung, W.-P. Kong, O. Schwartz, et al., "pH-dependent entry of severe acute respiratory syndrome coronavirus

- is mediated by the spike glycoprotein and enhanced by dendritic cell transfer through DC-SIGN," *Journal of virology*, vol. 78, pp. 5642-5650, 2004.
- [17] Y. Dong, T. Dai, Y. Wei, L. Zhang, M. Zheng, and F. Zhou, "A systematic review of SARS-CoV-2 vaccine candidates," *Signal transduction and targeted therapy*, vol. 5, pp. 1-14, 2020.
- [18] M. Kurokawa, H. Ochiai, K. Nagasaka, M. Neki, H. Xu, S. Kadota, et al., "Antiviral traditional medicines against herpes simplex virus (HSV-1), poliovirus, and measles virus in vitro and their therapeutic efficacies for HSV-1 infection in mice," *Antiviral research*, vol. 22, pp. 175-188, 1993.
- [19] H.-X. Xu, S. Kadota, M. Kurokawa, K. Shiraki, T. Matsumoto, and T. Namba, "Isolation and structure of woodorien, a new glucoside having antiviral activity, from *Woodwardia orientalis*," *Chemical and pharmaceutical bulletin*, vol. 41, pp. 1803-1806, 1993.
- [20] S. Kannan and P. Kolandaivel, "Antiviral potential of natural compounds against influenza virus hemagglutinin," *Computational biology and chemistry*, vol. 71, pp. 207-218, 2017.
- [21] H.-X. Xu, D.-S. Ming, H. Dong, and P. P.-H. BUT, "A new anti-HIV triterpene from *Geum japonicum*," *Chemical and pharmaceutical bulletin*, vol. 48, pp. 1367-1369, 2000.
- [22] Y.-B. Zhang, D. Luo, L. Yang, W. Cheng, L.-J. He, G.-K. Kuang, et al., "Matrine-type alkaloids from the roots of *sophora flavescens* and their antiviral activities against the hepatitis B virus," *Journal of natural products*, vol. 81, pp. 2259-2265, 2018.
- [23] J. Cinatl, B. Morgenstern, G. Bauer, P. Chandra, H. Rabenau, and H. Doerr, "Glycyrrhizin, an active component of liquorice roots, and replication of SARS-associated coronavirus," *The Lancet*, vol. 361, pp. 2045-2046, 2003.
- [24] M. F. Boni, P. Lemey, X. Jiang, T. T.-Y. Lam, B. W. Perry, T. A. Castoe, et al., "Evolutionary origins of the SARS-CoV-2 sarbecovirus lineage

- responsible for the COVID-19 pandemic,” *Nature microbiology*, vol. 5, pp. 1408-1417, 2020.
- [25] Y. Xian, J. Zhang, Z. Bian, H. Zhou, Z. Zhang, Z. Lin, et al., ”Bioactive natural compounds against human coronaviruses: a review and perspective,” *Acta Pharmaceutica Sinica B*, vol. 10, pp. 1163-1174, 2020.
- [26] Y. Chen, Q. Liu, and D. Guo, ”Emerging coronaviruses: genome structure, replication, and pathogenesis,” *Journal of medical virology*, vol. 92, pp. 418-423, 2020.
- [27] P. C. Woo, Y. Huang, S. K. Lau, and K.-Y. Yuen, ”Coronavirus genomics and bioinformatics analysis,” *viruses*, vol. 2, pp. 1804-1820, 2010.
- [28] S. Perlman and J. Netland, ”Coronaviruses post-SARS: update on replication and pathogenesis,” *Nature reviews microbiology*, vol. 7, pp. 439-450, 2009.
- [29] S. R. Weiss and S. Navas-Martin, ”Coronavirus pathogenesis and the emerging pathogen severe acute respiratory syndrome coronavirus,” *Microbiology and molecular biology reviews*, vol. 69, pp. 635-664, 2005.
- [30] N. Zhu, D. Zhang, W. Wang, X. Li, B. Yang, J. Song, et al., ”A novel coronavirus from patients with pneumonia in China, 2019,” *New England journal of medicine*, 2020.
- [31] I. d. A. Santos, V. R. Grosche, F. R. G. Bergamini, R. Sabino-Silva, and A. C. G. Jardim, ”Antivirals against coronaviruses: candidate drugs for SARS-CoV-2 treatment?,” *Frontiers in microbiology*, vol. 11, p. 1818, 2020.
- [32] K. Anand, S. Karade, S. Sen, and R. Gupta, ”SARS-CoV-2: camazotz’s curse,” *medical journal armed forces india*, vol. 76, pp. 136-141, 2020.
- [33] G. Simmons, P. Zmora, S. Gierer, A. Heurich, and S. Pöhlmann, ”Proteolytic activation of the SARS-coronavirus spike protein: cutting enzymes at the cutting edge of antiviral research,” *Antiviral research*, vol. 100, pp. 605-614, 2013.

- [34] J. P. Chambers, J. Yu, J. J. Valdes, and B. P. Arulanandam, "SARS-CoV-2, Early Entry Events," *Journal of Pathogens*, vol. 2020, p. 9238696, 2020/11/24 2020.
- [35] M. A. Tortorici and D. Veessler, "Structural insights into coronavirus entry," *Advances in virus research*, vol. 105, pp. 93-116, 2019.
- [36] M. Hoffmann, H. Kleine-Weber, S. Schroeder, N. Krüger, T. Herrler, S. Erichsen, et al., "SARS-CoV-2 cell entry depends on ACE2 and TMPRSS2 and is blocked by a clinically proven protease inhibitor," *cell*, vol. 181, pp. 271-280. e8, 2020.
- [37] A. G. Harrison, T. Lin, and P. Wang, "Mechanisms of SARS-CoV-2 transmission and pathogenesis," *Trends in immunology*, 2020.
- [38] S. Ghosh, T. A. Dellibovi-Ragheb, A. Kerviel, E. Pak, Q. Qiu, M. Fisher, et al., "Coronaviruses use lysosomes for egress instead of the biosynthetic secretory pathway," *Cell*, vol. 183, pp. 1520-1535. e14, 2020.
- [39] Y. M. Arabi, A. Alothman, H. H. Balkhy, A. Al-Dawood, S. AlJohani, S. Al Harbi, et al., "Treatment of Middle East respiratory syndrome with a combination of lopinavir-ritonavir and interferon-beta 1b (Miracle Trial): study protocol for a randomized controlled trial," *Trials*, vol. 19, pp. 1-13, 2018.
- [40] T. L. I. Diseases, "Challenges of coronavirus disease 2019," *The Lancet. Infectious Diseases*, vol. 20, p. 261, 2020.
- [41] D. Wu, T. Wu, Q. Liu, and Z. Yang, "The SARS-CoV-2 outbreak: what we know," *International Journal of Infectious Diseases*, vol. 94, pp. 44-48, 2020.
- [42] P. Hunziker, "Vaccination strategies for minimizing loss of life in Covid-19 in a Europe lacking vaccines," Available at SSRN 3780050, 2021.
- [43] S. A. Jassim and M. A. Najji, "Novel antiviral agents: a medicinal plant perspective," *Journal of applied microbiology*, vol. 95, pp. 412-427, 2003.

- [44] D. Hong-Zhi, H. Xiao-Ying, M. Yu-Huan, B.-S. Huang, and L. Da-Hui, "Traditional Chinese Medicine: an effective treatment for 2019 novel coronavirus pneumonia (NCP)," *Chinese journal of natural medicines*, vol. 18, pp. 206-210, 2020.
- [45] R. M. Romeilah, S. A. Fayed, and G. I. Mahmoud, "Chemical compositions, antiviral and antioxidant activities of seven essential oils," *Journal of Applied Sciences Research*, vol. 6, pp. 50-62, 2010.
- [46] J. S. Raut and S. M. Karuppayil, "A status review on the medicinal properties of essential oils," *Industrial crops and products*, vol. 62, pp. 250-264, 2014.
- [47] F. Bakkali, S. Averbeck, D. Averbeck, and M. Idaomar, "Biological effects of essential oils—a review," *Food and chemical toxicology*, vol. 46, pp. 446-475, 2008.
- [48] B. Teixeira, A. Marques, C. Ramos, C. Serrano, O. Matos, N. R. Neng, et al., "Chemical composition and bioactivity of different oregano (*Origanum vulgare*) extracts and essential oil," *Journal of the Science of Food and Agriculture*, vol. 93, pp. 2707-2714, 2013.
- [49] E. Grondona, G. Gatti, A. G. López, L. R. Sánchez, V. Rivero, O. Pessah, et al., "Bio-efficacy of the essential oil of oregano (*Origanum vulgare* Lamiaceae. Ssp. *Hirtum*)," *Plant foods for human nutrition*, vol. 69, pp. 351-357, 2014.
- [50] B. Imelouane, H. Amhamdi, J.-P. Wathelet, M. Ankit, K. Khedid, and A. El Bachiri, "Chemical composition and antimicrobial activity of essential oil of thyme (*Thymus vulgaris*) from Eastern Morocco," *Int. J. Agric. Biol*, vol. 11, pp. 205-208, 2009.
- [51] N. A. Singh, P. Kumar, and N. Kumar, "Spices and herbs: Potential antiviral preventives and immunity boosters during COVID-19," *Phytotherapy Research*, vol. 35, pp. 2745-2757, 2021.

- [52] M. N. I. Bhuiyan, J. Begum, N. Ch, and F. Akter, "Constituents of the essential oil from leaves and buds of clove (*Syzigium caryophyllatum* (L.) Alston)," *African Journal of Plant Science*, vol. 4, pp. 451-454, 2010.
- [53] J.-G. Xu, T. Liu, Q.-P. Hu, and X.-M. Cao, "Chemical composition, antibacterial properties and mechanism of action of essential oil from clove buds against *Staphylococcus aureus*," *Molecules*, vol. 21, p. 1194, 2016.
- [54] K. Jeena, V. B. Liju, N. Umadevi, and R. Kuttan, "Antioxidant, anti-inflammatory and antinociceptive properties of black pepper essential oil (*Piper nigrum* Linn)," *Journal of Essential Oil Bearing Plants*, vol. 17, pp. 1-12, 2014.
- [55] G. Singh, P. Marimuthu, C. Catalan, and M. DeLampasona, "Chemical, antioxidant and antifungal activities of volatile oil of black pepper and its acetone extract," *Journal of the Science of Food and Agriculture*, vol. 84, pp. 1878-1884, 2004.
- [56] N. N. Kasim, S. Ismail, N. Masdar, F. Hamid, and W. Nawawi, "Extraction and potential of cinnamon essential oil towards repellency and insecticidal activity," *International Journal of Scientific and Research Publications*, vol. 4, pp. 2250-3153, 2014.
- [57] J. Gruenwald, J. Freder, and N. Armbruster, "Cinnamon and health," *Critical reviews in food science and nutrition*, vol. 50, pp. 822-834, 2010.
- [58] B. Alizadeh Behbahani, F. Falah, F. Lavi Arab, M. Vasiee, and F. Tabatabaee Yazdi, "Chemical composition and antioxidant, antimicrobial, and antiproliferative activities of *Cinnamomum zeylanicum* bark essential oil," *Evidence-based complementary and alternative medicine*, vol. 2020, 2020.
- [59] K. Jeena, V. B. Liju, and R. Kuttan, "Antioxidant, anti-inflammatory and antinociceptive activities of essential oil from ginger," *Indian J Physiol Pharmacol*, vol. 57, pp. 51-62, 2013.

- [60] M. Höferl, I. Stoilova, J. Wanner, E. Schmidt, L. Jirovetz, D. Trifonova, et al., "Composition and comprehensive antioxidant activity of ginger (*Zingiber officinale*) essential oil from Ecuador," *Natural product communications*, vol. 10, p. 1934578X1501000672, 2015.
- [61] K. Amma, M. P. Rani, I. Sasidharan, and V. N. P. Nisha, "Chemical composition, flavonoid-phenolic contents and radical scavenging activity of four major varieties of cardamom," *Int J Biol Med Res*, vol. 1, pp. 20-24, 2010.
- [62] S. Goudarzvand Chegini and H. Abbasipour, "Chemical composition and insecticidal effects of the essential oil of cardamom, *Elettaria cardamomum* on the tomato leaf miner, *Tuta absoluta*," *Toxin reviews*, vol. 36, pp. 12-17, 2017.
- [63] I. Ogunwande, N. Olawore, K. Adeleke, and O. Ekundayo, "Chemical composition of essential oil of *myristica fragrans* houtt (nutmeg) from nigeria," *Journal of Essential Oil Bearing Plants*, vol. 6, pp. 21-26, 2003.
- [64] I. Kapoor, B. Singh, G. Singh, C. S. De Heluani, M. De Lampasona, and C. A. Catalan, "Chemical composition and antioxidant activity of essential oil and oleoresins of nutmeg (*Myristica fragrans* Houtt.) fruits," *International journal of food properties*, vol. 16, pp. 1059-1070, 2013.
- [65] G. Periasamy, A. Karim, M. Gibrelibanos, and G. Gebremedhin, "Nutmeg (*Myristica fragrans* Houtt.) oils," in *Essential oils in food preservation, flavor and safety*, ed: Elsevier, 2016, pp. 607-616.
- [66] Y. Kan, M. Kartal, T. Ozek, S. Aslan, and K. Baser, "Composition of essential oil of *Cuminum cyminum* L. according to harvesting times," *Turkish J. Pharm. Sci*, vol. 4, pp. 25-29, 2007.
- [67] M. Abdellaoui, E. d. T. Bouhlali, and L. E. Rhaffari, "Chemical composition and antioxidant activities of the essential oils of cumin (*Cuminum cyminum*) conducted under organic production conditions," *Journal of Essential Oil Bearing Plants*, vol. 22, pp. 1500-1508, 2019.

- [68] R. O. de Figueiredo, M. O. M. Marques, J. Nakagawa, and L. C. Ming, "Composition of coriander essential oil from Brazil," *Acta Horticulturae*, pp. 135-138, 2004.
- [69] A. A. Shahat, A. Y. Ibrahim, S. F. Hendawy, E. A. Omer, F. M. Hamouda, F. H. Abdel-Rahman, et al., "Chemical composition, antimicrobial and antioxidant activities of essential oils from organically cultivated fennel cultivars," *Molecules*, vol. 16, pp. 1366-1377, 2011.
- [70] J. Qiu, H. Li, H. Su, J. Dong, M. Luo, J. Wang, et al., "Chemical composition of fennel essential oil and its impact on *Staphylococcus aureus* exotoxin production," *World Journal of Microbiology and Biotechnology*, vol. 28, pp. 1399-1405, 2012.
- [71] L. P. Stanojevic, Z. R. Marjanovic-Balaban, V. D. Kalaba, J. S. Stanojevic, D. J. Cvetkovic, and M. D. Cakic, "Chemical composition, antioxidant and antimicrobial activity of basil (*Ocimum basilicum* L.) essential oil," *Journal of Essential Oil Bearing Plants*, vol. 20, pp. 1557-1569, 2017.
- [72] R. K. Joshi, "Chemical composition and antimicrobial activity of the essential oil of *Ocimum basilicum* L.(sweet basil) from Western Ghats of North West Karnataka, India," *Ancient science of life*, vol. 33, p. 151, 2014.
- [73] A. I. Hussain, F. Anwar, S. T. H. Sherazi, and R. Przybylski, "Chemical composition, antioxidant and antimicrobial activities of basil (*Ocimum basilicum*) essential oils depends on seasonal variations," *Food chemistry*, vol. 108, pp. 986-995, 2008.
- [74] M. M. Özcan and J. C. Chalchat, "Chemical composition and antifungal effect of anise (*Pimpinella anisum* L.) fruit oil at ripening stage," *Annals of Microbiology*, vol. 56, pp. 353-358, 2006.
- [75] B. Yabrir, A. Belhassan, T. Lakhlifi, G. Salgado M, M. Bouachrine, P. Munoz C, et al., "Minor composition compounds of algerian herbal medicines as inhibitors of SARS-CoV-2 main protease: Molecular docking and admet

- properties prediction,” *Journal of the Chilean Chemical Society*, vol. 66, pp. 5067-5074, 2021.
- [76] Y. Liu, M. Grimm, W.-t. Dai, M.-c. Hou, Z.-X. Xiao, and Y. Cao, ”CB-Dock: a web server for cavity detection-guided protein–ligand blind docking,” *Acta Pharmacologica Sinica*, vol. 41, pp. 138-144, 2020.
- [77] A. C. Wallace, R. A. Laskowski, and J. M. Thornton, ”LIGPLOT: a program to generate schematic diagrams of protein-ligand interactions,” *Protein engineering, design and selection*, vol. 8, pp. 127-134, 1995.
- [78] R. A. Laskowski and M. B. Swindells, ”LigPlot+: multiple ligand–protein interaction diagrams for drug discovery,” ed: ACS Publications, 2011.
- [79] F. Cheng, W. Li, Y. Zhou, J. Shen, Z. Wu, G. Liu, et al., ”admetSAR: a comprehensive source and free tool for assessment of chemical ADMET properties,” ed: ACS Publications, 2012.
- [80] J. H. Beigel, K. M. Tomashek, L. E. Dodd, A. K. Mehta, B. S. Zingman, A. C. Kalil, et al., ”Remdesivir for the treatment of Covid-19—preliminary report,” *New England Journal of Medicine*, vol. 383, pp. 1813-1836, 2020.
- [81] D. P. Rall, J. R. Stabenau, C. G. Zubrod, and J. Gaskins, ”Distribution of drugs between blood and cerebrospinal fluid: general methodology and effect of pH gradients,” *Journal of Pharmacology and Experimental Therapeutics*, vol. 125, pp. 185-193, 1959.
- [82] C. Kramer, A. Ting, H. Zheng, J. Hert, T. Schindler, M. Stahl, et al., ”Learning medicinal chemistry absorption, distribution, metabolism, excretion, and toxicity (ADMET) rules from cross-company matched molecular pairs analysis (MMPA) miniperspective,” *Journal of Medicinal Chemistry*, vol. 61, pp. 3277-3292, 2017.